Kennett, J.P., Baldauf, J.G., and Lyle, M. (Eds.), 1995
Proceedings of the Ocean Drilling Program, Scientific Results, Vol. 146 (Pt. 2)

8. CENTENNIAL-SCALE LATE QUATERNARY STRATIGRAPHIES OF CARBONATE AND ORGANIC CARBON FROM SANTA BARBARA BASIN, HOLE 893A, AND THEIR PALEOCEANOGRAPHIC SIGNIFICANCE[1]

James V. Gardner[2] and Peter Dartnell[2]

ABSTRACT

Stratigraphies of carbonate ($CaCO_3$) organic carbon (C_{org}), $CaCO_3$ and C_{org} mass accumulation rates (MAR), and paleoproductivity were determined with a sampling interval of 100 to 150 yr/sample for Ocean Drilling Program (ODP) Hole 893A from Santa Barbara Basin. Variations in $CaCO_3$ with time do not show the typical Pacific pattern (higher during glacial periods), nor any pattern that can be related to glacial-interglacial cycles. Variations in total C_{org} with time show four peaks of high values that occurred during Oxygen-Isotope Stage (OIS) 5 and earliest OIS-3. There is a moderate correlation between $CaCO_3$ and C_{org} mass accumulation rates. The fluxes of total sediment, $CaCO_3$, and C_{org} are all an order-of-magnitude higher than occurred on the adjacent open continental margin. Paleoproductivity values, a proxy derived from an empirical correlation with C_{org} MAR, approached 250 gC/m^2 yr during OIS-5 and OIS-1, and were ≤200 gC/m^2 yr during all other times. Surprisingly, only percentage C_{org} shows a response to global climatic forcing with a precessional periodicity of 23 k.y./cycle, but only during OIS-5. Basin isolation during periods of lowered sea levels appears to have regulated C_{org} and $CaCO_3$ deposition by a mechanism related to the advection of California Current and California Counter Current waters. Fluctuations in strength or dissolved-oxygen content of the basin's bottom water are documented in lamination cycles, but did not significantly affect the preservation of $CaCO_3$ and C_{org}.

INTRODUCTION

Ocean Drilling Program Site 893 was drilled just north of the center of Santa Barbara Basin (34°17.25′N, 120°02.19′W, 576.5-m water depth), the northern-most structural basin in the California borderland (Fig. 1). The floor of Santa Barbara Basin contains a thick, flat-lying sequence, the top 195 m of which is composed of interbedded intervals of laminated, non-laminated, and bioturbated sediment. Late Quaternary linear sedimentation rates in the basin generally exceeded 100 cm/k.y., which generated a very high-resolution continuous record of at least the past 161 k.y. Here, we investigate the total organic carbon (C_{org}) and carbonate ($CaCO_3$) stratigraphies of Hole 893A at a resolution of approximately 100 to 150 yr to determine if these two chemostratigraphic variables, or proxies derived from them, responded to global or local paleoceanographic or paleoclimatic forcing during the past 161 k.y.

Hole 893A recovered 21 Advanced Piston Cores comprising a complete section from the surface to 196.5-m sub-bottom. The recovered section represents the interval from about 161 ka to present with linear sedimentation rates that varied between about 100 and 150 cm/k.y. Hole 893A recovered sediments from four distinct lithofacies. The dominant recovered facies is an olive-gray laminated to bioturbated hemipelagic silty clay (Fig. 2) with variable, but small, amounts of diatoms, nannofossils, foraminifers, and radiolarians. Methane gas was common in the sediment throughout the drilling causing the cores to expand upon recovery which created artificial gaps in the section. Nannofossils dominate the biogenic carbonate fraction and smear slides reveal less than 5% detrital calcite, with only occasional traces of dolomite. Pyrite was commonly reported in smear slides, although rare (generally <2%) in abundance. Numerous gray interbeds occur throughout the section that contrast in color with the olive-gray hemipelagic silty clay. In addition, rare silty turbidites are scattered throughout the section.

Santa Barbara Basin is a 627-m-deep basin with sills at both the east and west ends (Fig. 1). The eastern sill is about 400 m above the basin floor and approximately 4 km wide, whereas the western sill is only 250 m high and about 3 km wide. The basin is approximately 50 km long and 25 km wide. The northern rim of the basin is the continental shelf, which varies in width from about 5 km at Point Conception to about 20 km in the vicinity of Santa Barbara. The southern rim of the basin is an island platform of the Santa Rosa-Cortez Ridge. The mountainous terrain north of Santa Barbara Basin rises to 1000 to 1500 m, whereas to the south the island platform rises only 500 m above present sea level.

The surface geomorphology of the region is commonly referred to as the Santa Barbara Channel. The only rivers that directly drain into Santa Barbara Channel are the Santa Clara and Ventura rivers (Fig. 1). Although the Santa Ynez River does not drain into Santa Barbara Channel, it does drain to the west onto the open continental margin where longshore drift is thought to transport some sediment to the south and southeast into Santa Barbara Basin (Fleischer, 1972).

The general surface circulation in Santa Barbara Channel today (Fig. 3) has been described as a slowly moving cyclonic eddy off the mainstream California Current that circulates between 34°30′N and 30°N as part of the Southern California Counter Current (Emery, 1960; Reid, 1965; Hickey, 1979; 1992). The cyclonic gyre is persistent throughout the year with the exception of the spring, when it is weak or absent. Upwelling on the open margin northwest of Santa Barbara Basin results from spring and summer northwesterly winds that force water offshore along the central California coast. Upwelled waters are advected south along the open margin by the California Current but some nutrient-rich water commonly turns shoreward and enters Santa Barbara Channel from the west (Hickey, 1992). The imported nutrient-rich waters support periods of enhanced productivity

[1]Kennett, J.P., Baldauf, J.G., and Lyle, M. (Eds.), 1995. *Proc. ODP, Sci. Results*, 146 (Pt. 2): College Station, TX (Ocean Drilling Program).
[2]U.S. Geological Survey, Menlo Park, CA 94025, U.S.A.

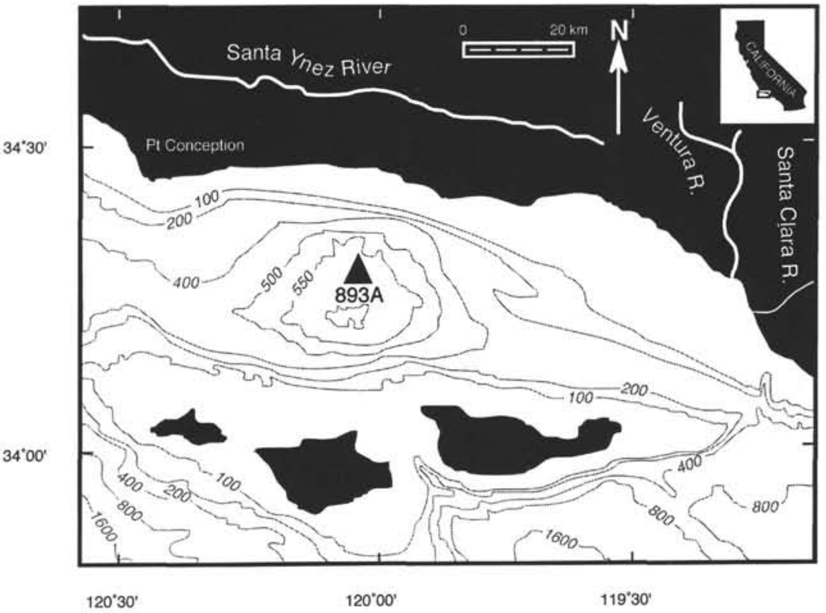

Figure 1. Modern generalized bathymetry (in meters) of Santa Barbara Basin and adjacent area.

in the basin region. In addition, it is thought that during upwelling conditions, cool, saline waters formed around Point Conception periodically invade and ventilate Santa Barbara Basin with oxygenated waters (Emery, 1960; Emery and Hülsemann, 1962; Sholkovitz and Gieskes, 1971; Reimers et al., 1990). Fall and winter months are dominated by southwesterly winds that bring warm, nutrient-depleted surface waters from the south into the basin that support only modest productivity and inhibit significant upwelling along the open margin. Fall and winter are also the seasons of major precipitation and large storm events. Pacific Intermediate Water and the open-ocean oxygen-minimum zone, which occupy a depth range of about 500–1200 m (summarized from data in the CalCOFI data reports) are restricted from entering the basin by the shallow western sill of Santa Barbara Basin (440 m). Under non-upwelling conditions, the water column of the basin is stratified from the depth of the western sill to the bottom, with concentrations of bottom-water dissolved oxygen that vary from 0.1 to 0.3 mL/L (Sholkovitz and Gieskes, 1971), concentrations low enough to limit burrowing benthic organisms and allow the seasonal sedimentation patterns to be preserved as annually laminated (varved) sequences.

It has long been known that the sediments of Santa Barbara Basin contain at least four different facies; laminated intervals, gray layers, silty turbidites, and the background hemipelagic olive-gray silty clays. The laminations have been described by various workers including Emery (1960), Emery and Hülsemann (1962), Fleischer (1972), Soutar and Crill, (1977), Soutar et al. (1977), and Reimers et al. (1990) and have been demonstrated to be varves. The gray layers have been discussed by Hülsemann and Emery (1961), Fleischer (1972), Drake et al. (1972), Soutar and Crill, (1977), Thornton (1984; 1986), and Pisias (1978) and the consensus of opinions is they represent flood deposits. Thornton (1984; 1986) describes turbidites and mass-flow deposits that fringe the basin floor. The hemipelagic silty clays represent bioturbated mixtures of laminated and some gray-layer sediment.

METHODS

Hole 893A was sampled for this study at 20-cm intervals throughout the entire 196.5-m length. The samples reported on here are offset by 10 cm from the samples analyzed and reported by Stein and Rack (this volume). The 20-cm sampling scheme provides a resolution of 100 to 150 yr/sample. Samples were collected from gray layers and sands as well as from the hemipelagic silty clay so that comparisons could be made between the various lithologies. Sample depths were adjusted for the gas-expansion voids using the depth-correction tables of Rack and Merrill (this volume).

Samples were oven dried at 60°C, powdered and analyzed for weight percentages of total carbon (TC) and inorganic carbon (IC) using a UIC Coulometric model 5010 carbon dioxide coulometer (Engleman et al., 1985). Organic carbon (C_{org}) was calculated as the difference (TC–IC), and $CaCO_3$ was calculated as

$$CaCO_3 = IC \times 8.33. \quad (1)$$

The accuracy of this method, determined from replicate standards, is 0.10 wt% ($1\sigma = 0.079$) for TC and 0.10 wt% ($1\sigma = 0.084$) for IC. As of this writing, the only data available concerning the contribution of terrestrial carbon vs. marine carbon to the total organic carbon in Hole 893A are C/N ratios and Rock-Eval parameters (R. Stein, pers. comm., 1994). Because neither of these techniques provide an unequivocal determination of the amount of marine vs. terrestrial C_{org}, we have chosen to only discuss *total* organic carbon. An example of analytical $CaCO_3$ and C_{org} data is shown in the Appendix and the complete data are included in the CD-ROM accompanying this volume. Complete data also are available upon request from the Data Librarian, Ocean Drilling Program, Texas A&M University, College Station, TX.

Because organic matter partially decomposes during deposition and burial, the amount of C_{org} preserved in the sediment is some function of the rate of production of organic matter, sediment and organic-matter composition (Müller and Suess, 1979; Berner, 1982; Emerson, 1985; Emerson et al., 1985; Sarnthein et al., 1987; 1988; Martin and Bender, 1988), pore-water composition, and a time-dependent rate of decomposition (Middelburg, 1989). Environments of slow sedimentation rates and low concentrations of C_{org} should allow decomposition of all labile C_{org} so that at a few meters depth C_{org} should reach some minimum value that represents the amount of the residual refractory C_{org}. However, in environments of relatively fast sedimentation rates and high concentrations of C_{org}, not all of the metabolizable C_{org} is decomposed before burial below the depth of active diagenesis. Santa Barbara Basin represents an extreme example of the second

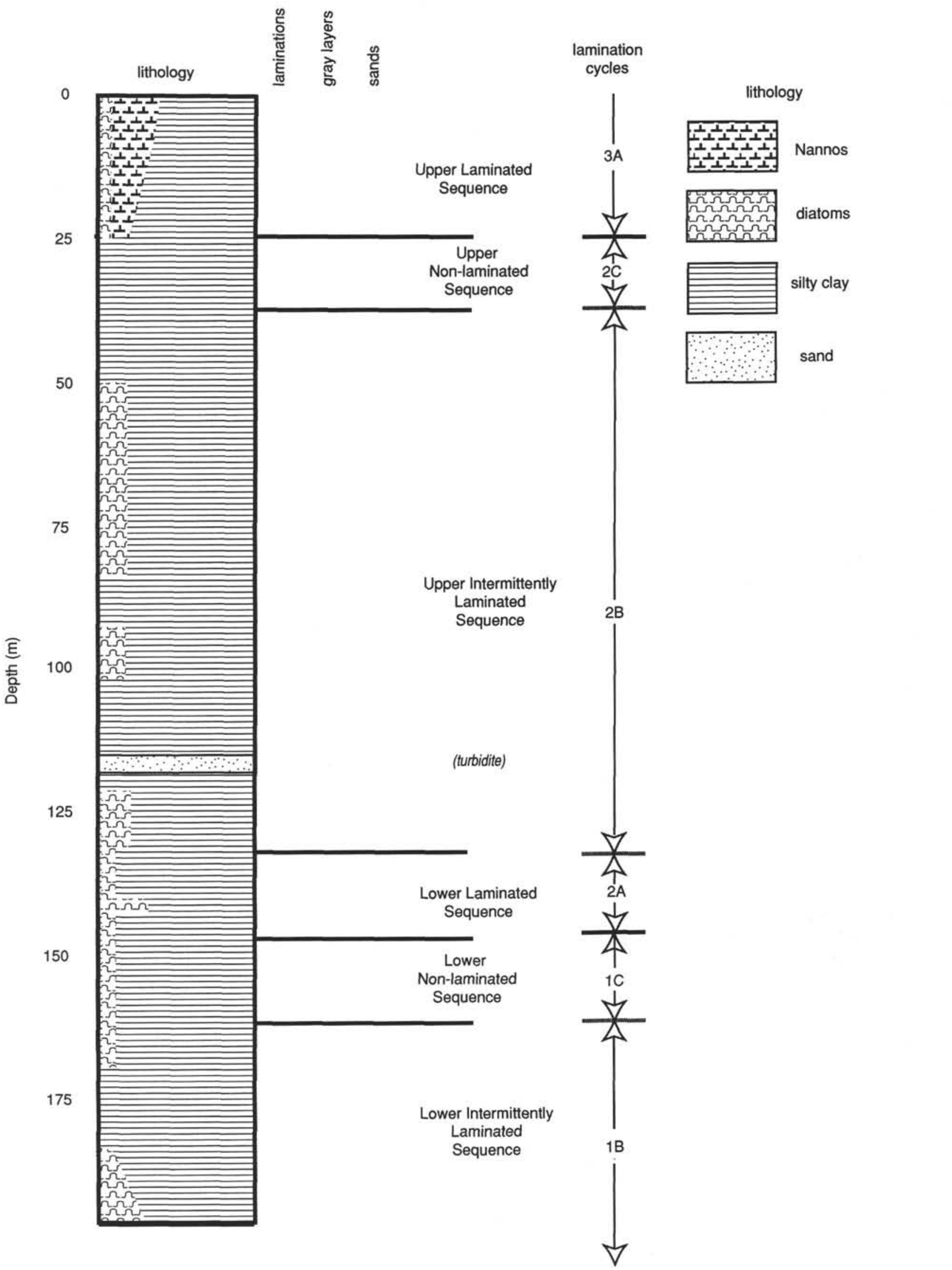

Figure 2. Generalized lithostratigraphy of Hole 893A with indication of biogenic contributions, locations of lamination cycles, gray layers, and sand interbeds.

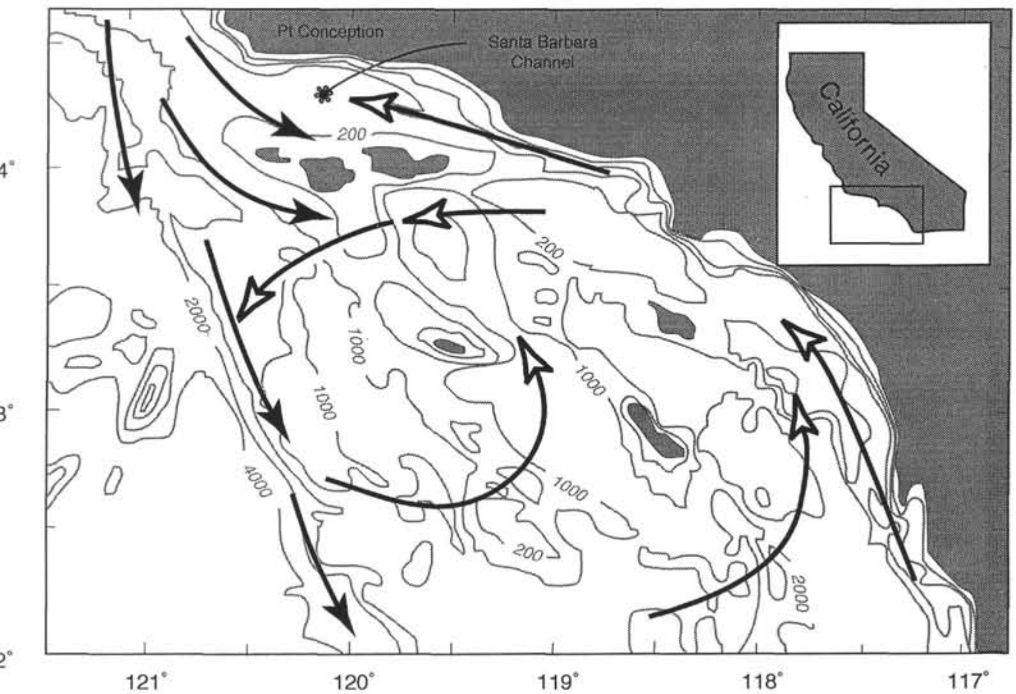

Figure 3. Generalized surface circulation in the California borderland (after Hickey, 1992). Solid arrowheads = California Current; open arrowheads = California Counter Current. Notice that both currents influence circulation in Santa Barbara Channel. Depth contours in meters.

case. Although there is no consensus as to how quickly diagenesis occurs during burial (see discussion in Lyle et al., 1992), this effect must be taken into account before C_{org} values within the zone of diagenesis can be directly compared to values collected below the zone. We developed a simple model for C_{org} decomposition based only on the observed decrease in C_{org} in the top of the section because organic-geochemistry and pore-water data from Hole 893A are not yet available and no studies of such data from long cores with comparably fast accumulation rates have been published. C_{org} values in Hole 893A show a pronounced exponential decrease from the surface to about 13 m sub-bottom (ca. 10 ka) where the values become asymptotic to a general minimum value (ca. 1.7%) that, for simplicity, we assume represents the remaining refractory components of C_{org} (Fig. 4). Heath et al. (1977) found a similar decrease in a piston core from Santa Barbara Basin. The observed exponential decrease of C_{org} can be modeled in the simple form of:

$$C = C_r + C_o e^{-kt} \qquad (2)$$

where C is the C_{org} (after decomposition) at time t, C_o is the initial C_{org} content, C_r is the 1.7% refractory C_{org}, and k is the decay rate. This model assumes that the exponential decay of C_{org} at the top of the core is the result of decomposition of labile C_{org}, and not a result of an exponential increase in productivity with time. Changes in productivity are preserved as the variance about the exponential trend and fluctuations about the 1.7% value below the depth of active decomposition. The C_{org} content at the surface of Hole 893A is approximately 3% and exponentially decays to a value of 1.7% at about 10 ka (Fig. 4). To mathematically decompose the excess C_{org} in the top of the section, we generated an age model for the core using the chronostratigraphy discussed below and calculated interval sedimentation rates. We interpolated the age of each sample and plotted log C_{org} vs. age to determine a decay rate (k) of 5.4 (10^{-5}) %/yr with an observed half life of approximately 7 k.y. We then used this decay rate to calculate, using Equation 2, the decomposition of C_{org} for each sample from the top of the section down to the depth of the 10 ka datum.

The chronostratigraphy used to generate the age model for Hole 893A (Table 1) is from 14 globally and regionally corrected AMS ^{14}C dates and 6 oxygen-isotope stage (OIS) boundaries determined by Ingram and Kennett (this volume) and Kennett (this volume), respectively. All ages are reported here in calendar year.

Bulk mass accumulation rates (MAR) were calculated as the product of the dry bulk density (DBD) (Rack et al., this volume) and the calculated sample-to-sample interval sedimentation rates interpolated from the above age model. The MARs of $CaCO_3$ and C_{org} were calculated as the product of the fraction of each component and the bulk MAR.

An equation for new productivity (interchangeably called paleoproductivity) was derived from the data of Sarnthein et al. (1988). The equation used by Sarnthein et al. (1988, their equation 1) could not be used because of an inconsistency between their variable units and their equation. However, they do provide their primary data so that an empirical regression can be made between C_{org} MAR and measured new productivity. The regression yields the equation:

$$P_{new} = 138.387 \times C^{0.436} \qquad (3)$$

where P_{new} is the paleoproductivity in gC/m^2 yr and C is C_{org} MAR in g/cm^2 k.y. The correlation coefficient of the regression equation is 0.872 (Fig. 5).

RESULTS

Hemipelagic Sediment

Plots of percent $CaCO_3$ and C_{org} vs. corrected depth and age are shown in Figures 6 and 7, respectively. The plots vs. depth include all

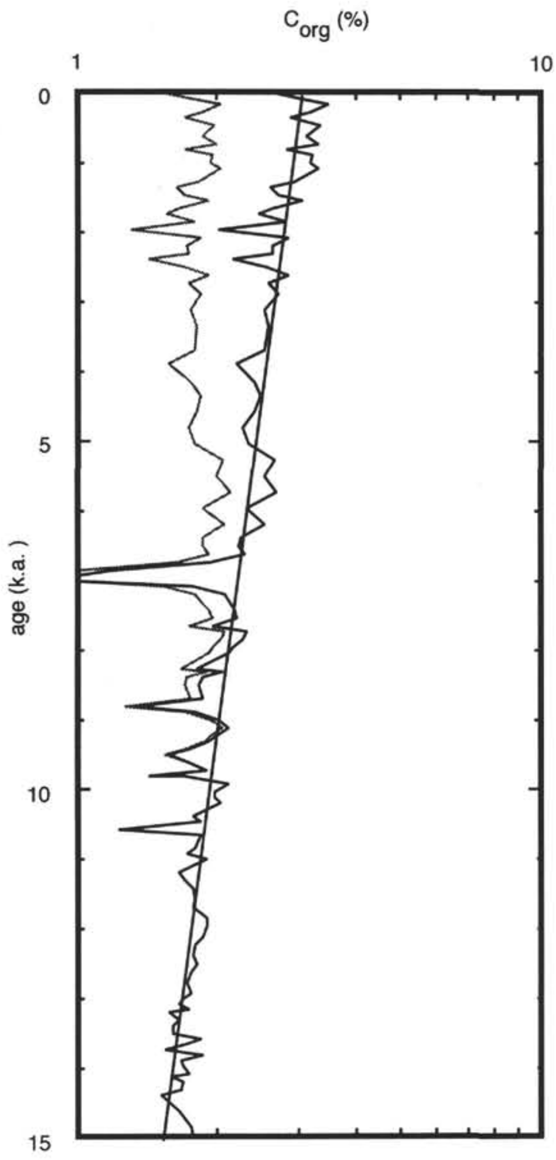

Figure 4. Semi-log plot of top 15 k.y. of percent C_{org} (black line) and percent C_{org} after mathematical decomposition (gray line) vs. age for Hole 893A. Exponential regression has the form $C = C_r + C_o e^{-kt}$ where C_r is the percent refractory C_{org}, C is the decomposed C_{org} value, C_o is the measured C_{org} value, k is the decay rate, and t is the age, in k.y. The correlation coefficient is 0.75.

the samples, regardless of whether they were collected from a gray layer, a turbidite, or the hemipelagic silty clay. Carbonate percentages vary from a maximum of 14.6% to a minimum of 0% with a mean of 5.9% and standard deviation of 2.3%. Average carbonate percentages show relatively constant values of ~7% from near the bottom of the hole to about 158-m sub-bottom. This is followed by an interval of steadily decreasing average $CaCO_3$ to 122 m sub-bottom to average values of ~3% with considerable high-frequency variability superimposed on the decrease. Average $CaCO_3$ values remain ~3% to 112 m sub-bottom where they rapidly increase to ~5% by 106 m sub-bottom. The average $CaCO_3$ values remain at ~5% with low variability until 50 m sub-bottom where a general increase begins to ~10% at the top of the hole. This last increase in mean $CaCO_3$ values is interrupted by a well-defined reduction that occurs between 29 and 19 m sub-bottom. $CaCO_3$ variability shows a pronounced plateau of high values from about 18 m to the top of the section.

Table 1. Chronostratigraphic datums used to develop age model for Hole 893A.

Depth (m)	Age (ka)	Type
0	0	
3.62	1.67	^{14}C
5.67	2.78	^{14}C
8.71	6.19	^{14}C
13.97	9.34	^{14}C
16.84	10.79	^{14}C
17.60	11.06	^{14}C
18.75	11.82	^{14}C
20.39	12.971	^{14}C
21.94	13.436	^{14}C
24.12	14.411	^{14}C
25.58	16.267	^{14}C
29.61	18.254	^{14}C
31.52	2.792	^{14}C
43.17	28.896	^{14}C
73.89	51.000	OIS
90.49	65.000	OIS
140.69	116.000	OIS
147.46	122.560	OIS
156.87	127.000	OIS
195.00	161.340	OIS

Notes: All ^{14}C ages were determined by accelerator mass spectrometry, are corrected for both global and regional reservoir differences, and are reported in calendar years (Ingram and Kennett, this volume); OIS = oxygen-isotope stage boundaries (after Kennett, this volume).

Organic carbon (after decomposition) (Fig. 7) only varies between 3.8% and 0.6%, (mean = 1.7%, standard deviation = 0.3%). C_{org} shows relatively low average values (~1.5%) and low variability at the bottom of the section to about 150-m sub-bottom, followed by three distinct and one less-distinct intervals of high C_{org}, each decreasing in amplitude, that occur at 149.5 to 136 m, 134 to 116 m, 108 to 94.5 m, and 82 to 68 m sub-bottom. The three deeper peaks show higher variability in C_{org} than does the rest of the section. The analytical data of Stein and Rack (this volume) suggest to them that marine C_{org} dominates the organic carbon in these peak intervals. Thereafter, average values of C_{org} show a gradual increase from about 88 m to the top of the section.

To better understand the "normal" (non-event) sedimentation and to compare normal sedimentation to events, such as gray layers and sandy turbidites, we determined the depths of all gray layers and sands from black and white photographs and color 35-mm slides of the cores. The event intervals are essentially instantaneous events so they were subtracted from the sediment sequence in the same way that gas voids were eliminated. An age model was then generated by linearly interpolating the age of each sample using sedimentation rates derived between each chronostratigraphic datum. When the sample ages are used to generate an interval sedimentation rate model, several suspiciously large increases occur in interval sedimentation rates (Fig. 8). The large fluctuations in interval sedimentation rates in the top 20 k.y. of the section are controlled by 14 corrected AMS ^{14}C ages and are considered reliable. The abrupt 100% increase in sedimentation rates at 127 ka is a result of the location of the OIS-6/5 boundary from the oxygen-isotope curve (Kennett, this volume; Ingram and Kennett, this volume). The oxygen-isotope curve clearly defines the OIS-6/5 boundary so the age assignment appears reliable. However, because there are no commensurate changes in dry bulk density, percent $CaCO_3$ or percent C_{org} at this interval, as one might expect if the sedimentation rate increased by a factor of two, we think this large increase in sedimentation rate is suspicious, and we will not interpret changes in this interval.

Clearly, when plotted vs. age (Fig. 6B), the carbonate stratigraphy at Hole 893A does not follow the typical Pacific glacial-interglacial carbonate pattern of high carbonate in glacial intervals and low car-

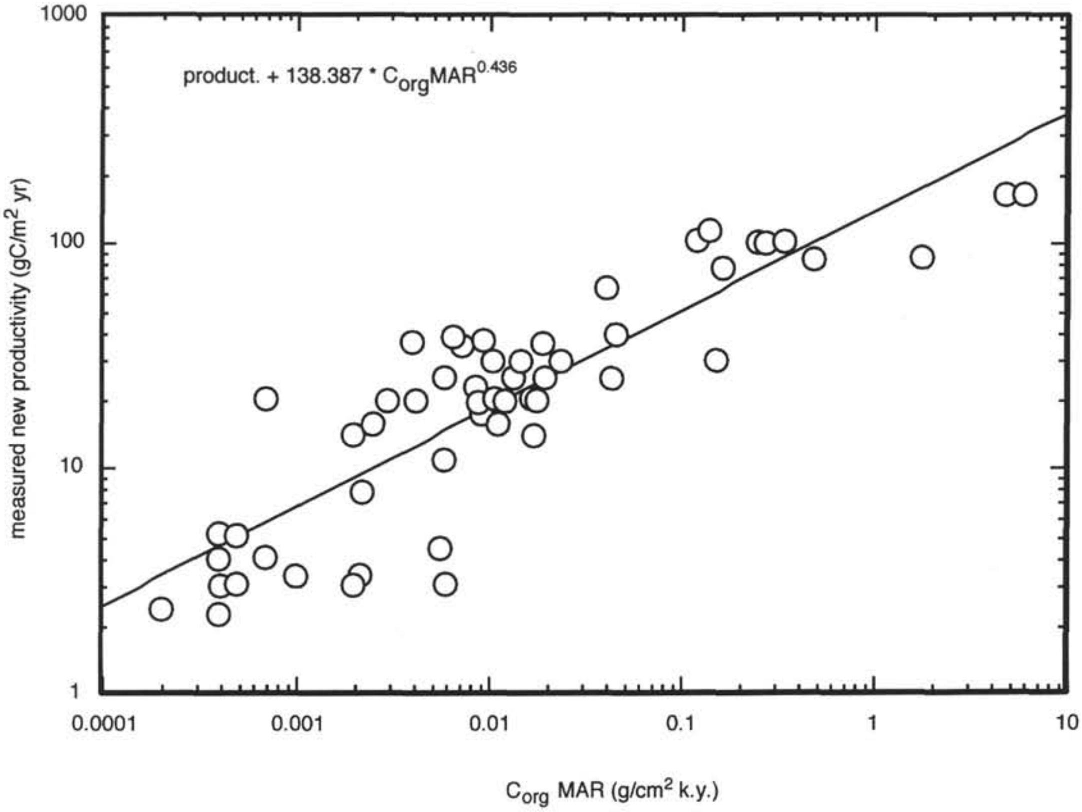

Figure 5. Plot of measured new productivity vs. C_{org} MAR. Data from Sarnthein et al. (1988).

bonate in interglacial intervals, first described by Arrhenius (1952) and by many others since. Similarly, C_{org} (Fig. 7B) appears to fluctuate because of something other than glacial-interglacial forcing. A paired t-test analysis performed on the means of C_{org} and $CaCO_3$ for each of the oxygen-isotope stages, as delimited by Martinson et al. (1987), shows no consistent similarities in mean values of C_{org} or $CaCO_3$ in glacial or interglacial oxygen-isotope stages.

The four pulses of high C_{org} concentration each have a duration of ~10 k.y., and the oldest three occurred during OIS-5, whereas the youngest occurred during early OIS-3 (Fig. 7B). C_{org} event 1 occurred between 123 and 112 ka, event 2 between 103 and 92 ka, event 3 between 83 and 74 ka, and event 4 between 59 and 48 ka. At no other time in the record did C_{org} sustain the high values (>2.5%) of the pulses, nor were there any other comparably long periods of elevated-C_{org} values. Calculations of the standard deviations from the mean show that the three oldest intervals of the events were also the periods of the highest fluctuations of C_{org}. The lack of similarity in variability suggests that the youngest pulse event may be unrelated to the older three pulses. Cross-spectral analysis of percent $CaCO_3$ and percent C_{org} shows little covariation (maximum $r = -0.30$ at 2000-yr lag) between the two variables over a ±10 k.y. shift (Fig. 9), demonstrating that the two variables are independent of one another. Even the trends in percent $CaCO_3$ show no covariation with $\%C_{org}$ during glacial-interglacial cycles. Glacial OIS-6 and OIS-2 have similar $CaCO_3$ statistics with values consistently above the mean for the record. Values of $CaCO_3$ during glacial OIS-4 and interstadial OIS-3 are similar but with values consistently below the mean, whereas $CaCO_3$ values during glacial OIS-6 are different from those from OIS-4. Interglacial OIS-5 has the lowest values of $CaCO_3$, yet interglacial OIS-1 has the highest values. A $CaCO_3$ event occurred during OIS-2 between 18 and 11 ka that shows up as a distinctive zone of low values that appear to interrupt a rapid increase of $CaCO_3$ that began during the latest OIS-3 at about 30 ka. The three glacial periods (OIS-6, 4, and 2) have relatively dissimilar $CaCO_3$ trends as do the three interglacial periods. Consequently, it appears some forcing other than global climate must be modulating $CaCO_3$ and C_{org}.

The recovered lithology also can be subdivided into one complete lamination cycle and two incomplete lamination cycles: a cycle consisting of a laminated interval, followed by an intermittently laminated interval, which in turn is followed by a non-laminated section (Fig. 2). However, there do not appear to be any trends in C_{org} or $CaCO_3$ percentages that correspond with these lithologic cycles (Figs. 6 and 7). Comparative statistics using a paired t-test analysis show that there are no statistical similarities between similar intervals in different lamination cycles.

Gray Layers and Sands

Data from 30 analyzed gray layers were separated out and statistically compared with data from the hemipelagic olive-gray silty clay. Together, the gray layers have an average C_{org} value of 1.50% and an average $CaCO_3$ value of 3.78%, whereas the hemipelagic olive-gray facies has average values of 1.74% and 5.90% for C_{org} and $CaCO_3$, respectively. Pisias (1978) found similar $CaCO_3$ and C_{org} values when comparing gray layers and the hemipelagic olive-gray facies in the youngest 8 k.y. of the section. Paired t-tests between the mean $CaCO_3$ and C_{org} values of the gray layers vs. the hemipelagic facies show the gray layers to be statistically different at the 95% level. The maximum value for $CaCO_3$ in the hemipelagic facies is 19.59%, whereas the maximum value in the gray layers is only 6.89%, although the minimum $CaCO_3$ values for the two facies are comparable. Interestingly, the minimum values of C_{org}, dominated by terrestrial C_{org} (Stein and Rack, this volume), may be more indicative of different sources. The minimum value of C_{org} in the hemipelagic facies is 0.15%, whereas it is 0.89% in the gray layers. This suggests the two facies are derived from different sources.

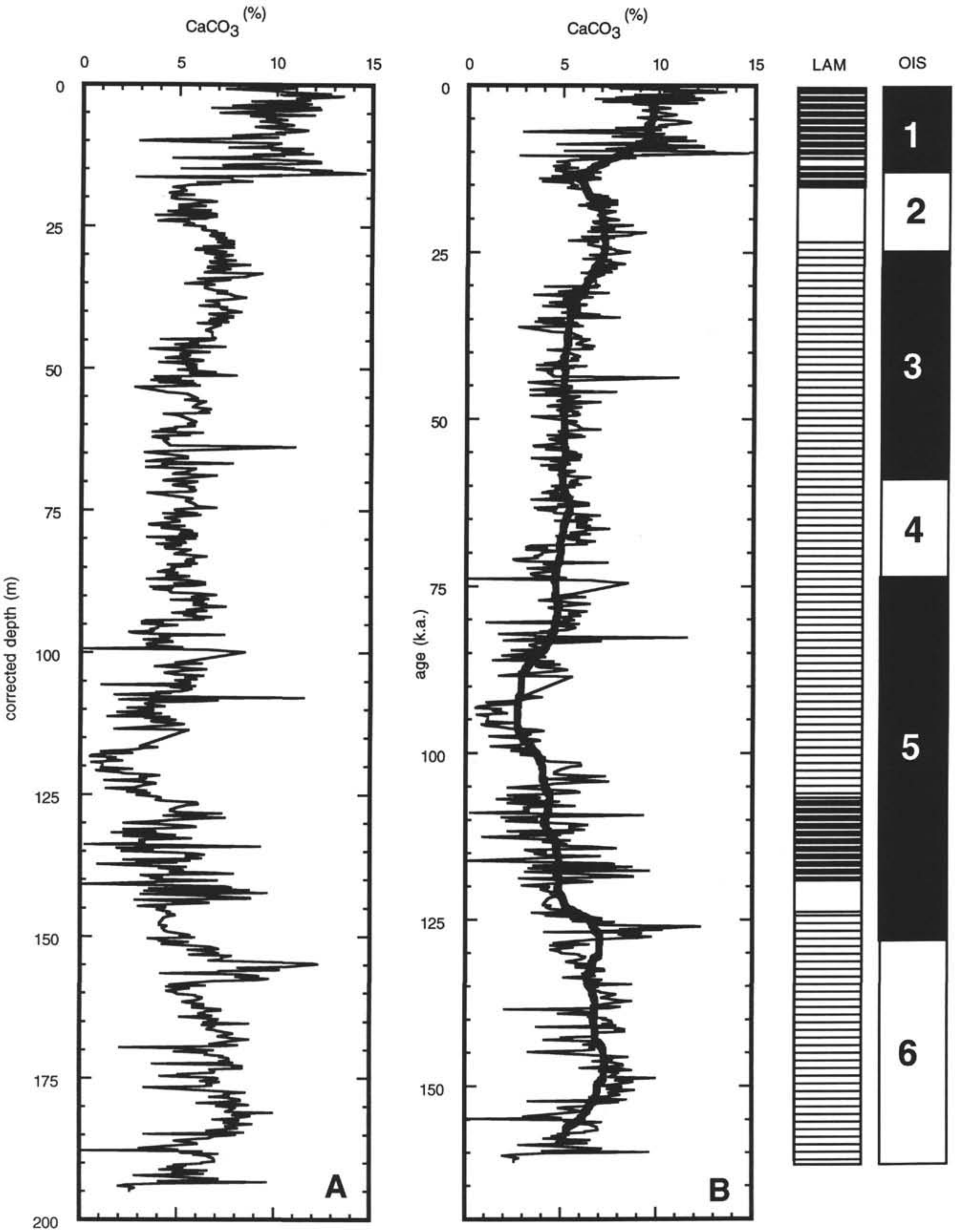

Figure 6. $CaCO_3$ percentages plotted vs. depth (**A**) and age (**B**) for Hole 893A. The smoothed curve is a 51-point running average. Column labeled "OIS" shows Oxygen-Isotope Stages, and column labeled "LAM" shows laminated sequences with heavy horizontal lines, intermittently laminated sequences with light horizontal lines, and nonlaminated sequences with no horizontal lines. The two right-hand columns are plotted vs. age.

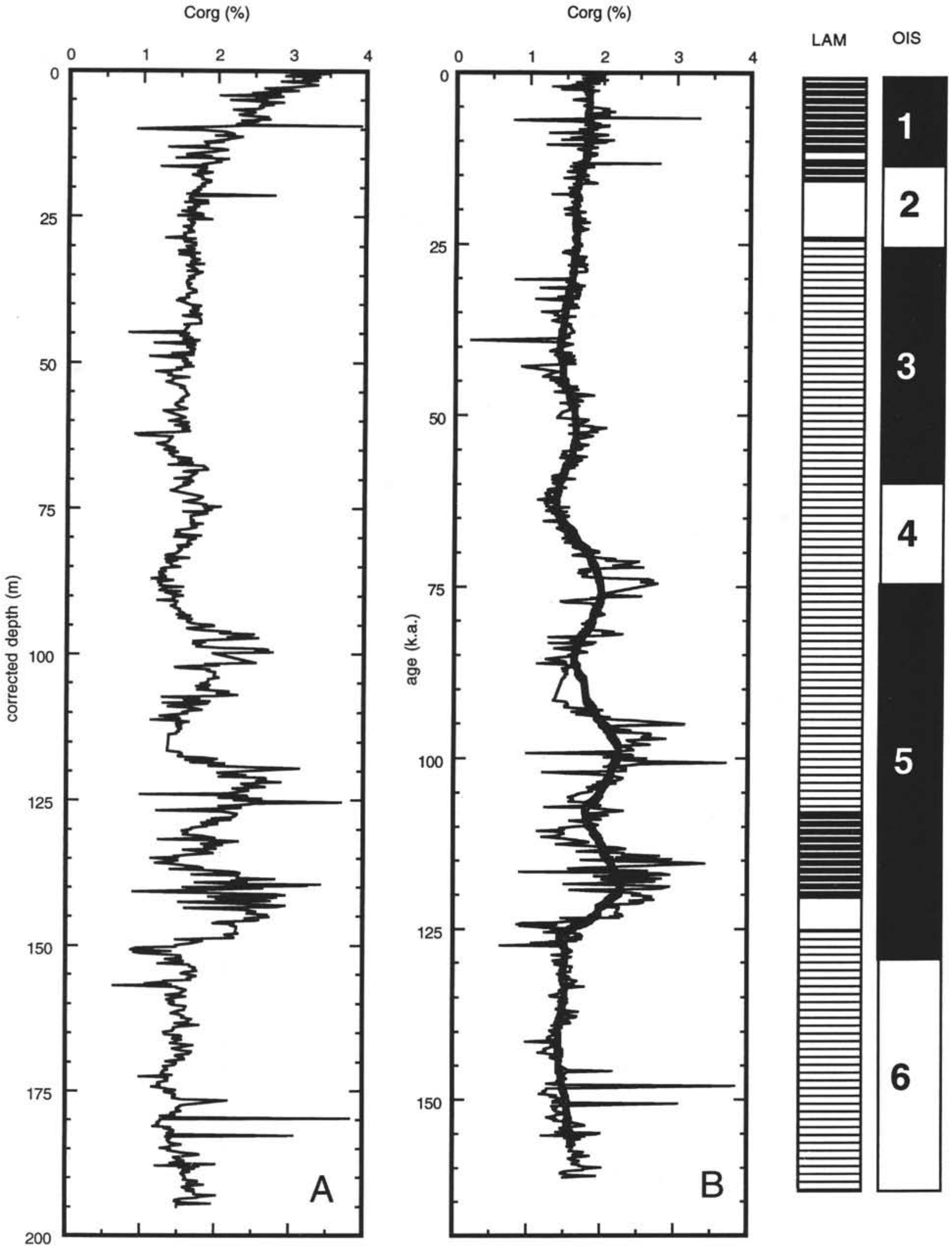

Figure 7. Analytical C_{org} percentages plotted vs. depth (**A**) and C_{org} after decomposition vs. age (**B**). The smoothed curve is a 51-point running average. See Figure 6 caption for explanation of far-right columns, which are plotted vs. age.

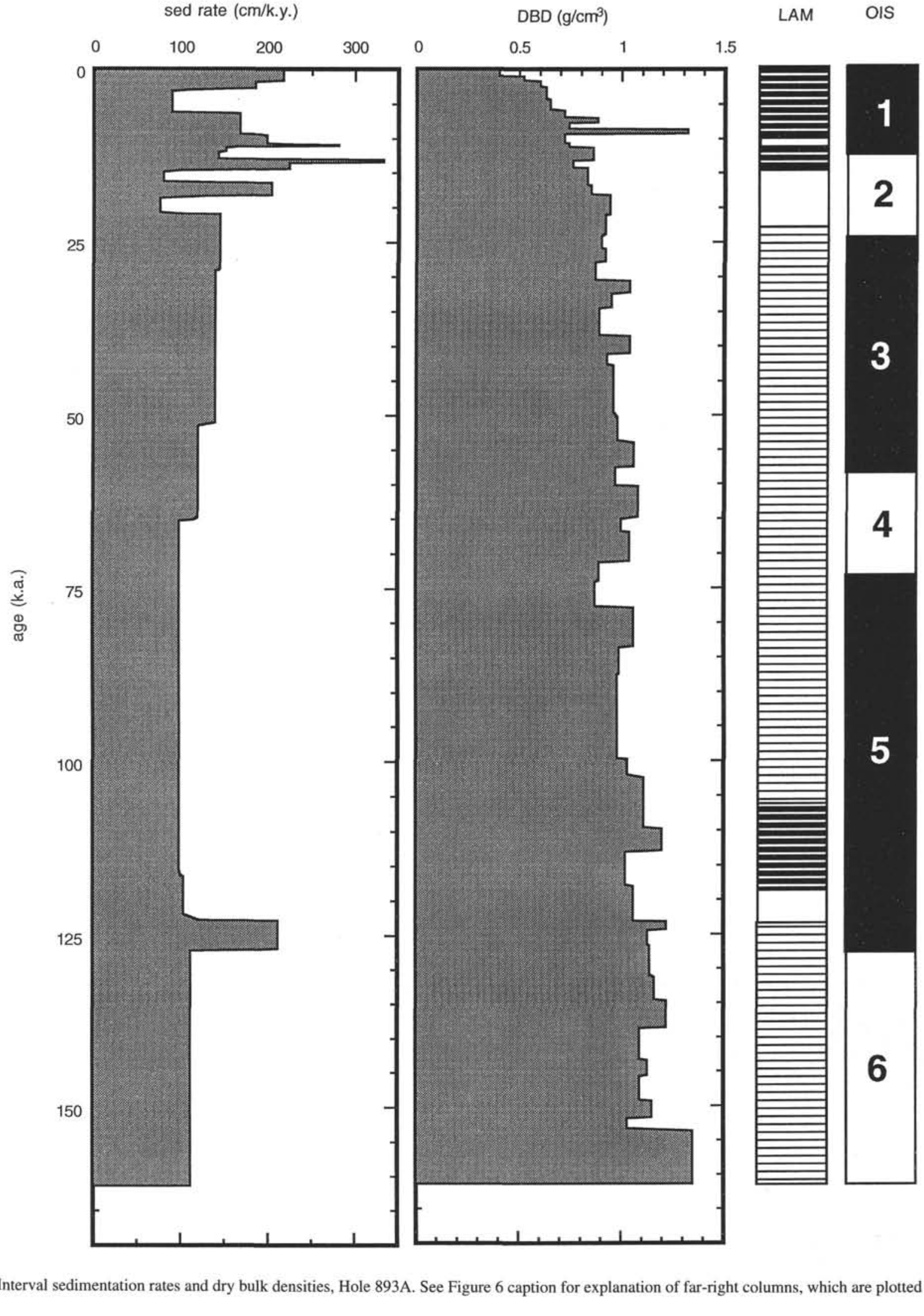

Figure 8. Interval sedimentation rates and dry bulk densities, Hole 893A. See Figure 6 caption for explanation of far-right columns, which are plotted vs. age.

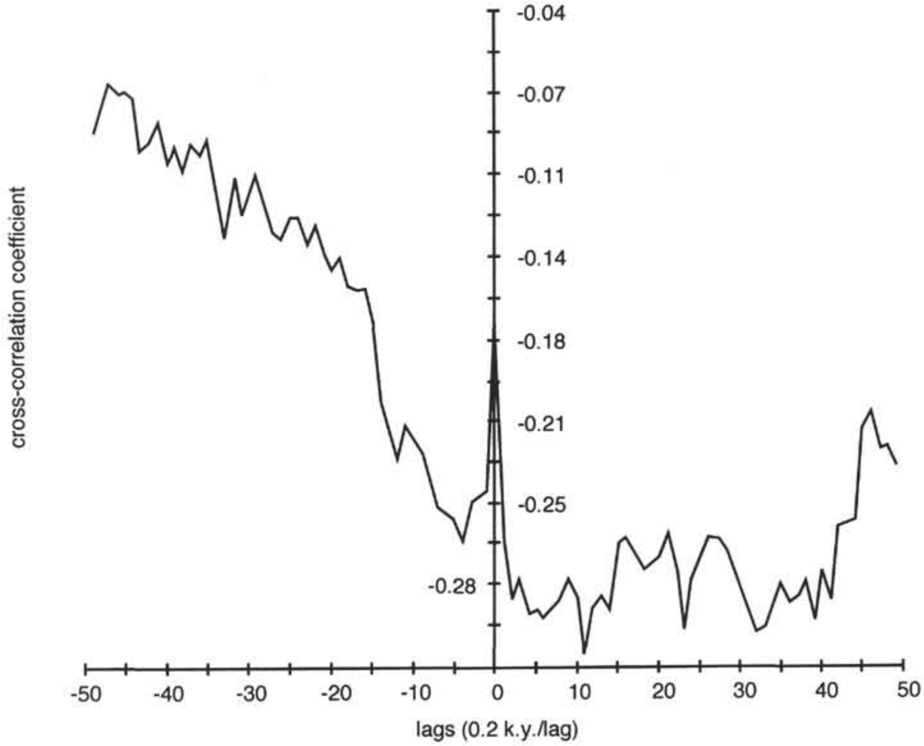

Figure 9. Cross-correlation coefficients between percent $CaCO_3$ and percent C_{org} over ± 10 k.y. shifts at 0.2 k.y./shift.

DISCUSSION

Santa Barbara Basin and its environment is not analogous to the deep sea, where numerous studies of C_{org} and $CaCO_3$ have been made over the past few decades. Santa Barbara Basin is a near-shore, shallow, silled basin with anoxic to suboxic bottom-water conditions that have prevailed over most of the past 161 k.y. In addition, undoubtedly a significant amount of the C_{org} must be terrestrial, rather than marine in origin, as suggested by the extremely fast sedimentation rates even though the data of Stein and Rack (this volume) suggest that marine C_{org} is equal to or dominant over terrestrial C_{org} throughout much of the recovered section. We lack values of biogenic opal to complete the analyses of the biogenic components and to allow us to calculate the amount of terrigenous input relative to the biogenic fluxes. Because of these uncertainties and the lack of available quantitative chromatographic organic-geochemical analyses to determine the partitioning of C_{org} between terrestrial and marine sources, we are cautious at this stage in our interpretations of C_{org} and proxies derived from C_{org} in Santa Barbara Basin. Much of the current literature on the relationships between C_{org}, $CaCO_3$, and productivity in the deep sea may not be strictly relevant to Santa Barbara Basin. However, because so much work has been done on these relationships in deep-sea sediments, it is instructive to compare the sediments of Santa Barbara Basin with results from the deep sea.

Mass Accumulation Rates

Analyzing stratigraphic variations from parameters such as C_{org} and $CaCO_3$ from weight percentages often obscures the actual trends in sedimentation because of the assumed closed system and the effects of dilution. Mass accumulation rates (weight/unit area/unit time) can be calculated, but only if reliable dry bulk density (DBD), calculated from measured wet bulk densities, and numerous age datums are available. Fortunately, Hole 893A has very reliable DBD values (Fig. 8) but unfortunately only 20 age datums (Table 1). The interval of 0 to 28 ka is fairly well dated with 14 AMS dates, but then the chronostratigraphy is only constrained by correlation to the standard oxygen-isotope curve of Martinson et al. (1987). Within the constraints of constant sedimentation rate between dated intervals, mass accumulation rates (MAR) can be calculated, sample-for-sample, for the entire recovered section (Fig. 10). Measured wet-bulk densities increase in the top 20 k.y. of the section in a fairly smooth, predictable trend, but remain almost uniform for the lower 140 k.y. of the section (Rack et al., this volume). Consequently, bulk MARs are modulated more by the interval sedimentation rates, which vary considerably (Fig. 8), than by DBD. The pattern of C_{org} MAR at Hole 893A reflects the pattern of percent C_{org} with the exception of high-frequency variability in the Holocene. The same general patterns are found in C_{org} MARs and $CaCO_3$ MARs for the entire record as are found in $\%C_{org}$ and $\%CaCO_3$, respectively. Cross-correlation analysis of $CaCO_3$ MAR against C_{org} MAR shows a moderate maximum covariation ($r = 0.48$) with no lags (Fig. 11), and virtually no correlations at any lags over the range of ±10 k.y. at 0.2 k.y./lag. This suggests that, overall, the mass accumulation rates of $CaCO_3$ and C_{org} also are independent of one another, just as was found for $\%CaCO_3$ and $\%C_{org}$. However, when linear regressions between percentages of C_{org} and $CaCO_3$ and C_{org} and $CaCO_3$ MARs in the various lithofacies are run, the Upper Nonlaminated Sequence and the Upper Laminated Sequence show high correlations in MARs (0.94 and 0.63, respectively; Table 2) These high correlation coefficients suggest that terrigenous fluxes in these two intervals were minimal compared to the other lithofacies and that $CaCO_3$ and C_{org} fluxes are interrelated in these two intervals.

The fast accumulation rates in Santa Barbara Basin are the result of high fluxes of both terrigenous and biogenic components. Bulk MARs, C_{org} MAR, and $CaCO_3$ MAR for Santa Barbara Basin average an order-of-magnitude higher than values on the adjacent continental margin off Point Conception (Gardner, unpubl. data) and in other open-margin areas (Sarnthein, et al., 1987). Consequently, fluxes of both terrestrial detritus *and* biogenic debris were much higher in Santa Barbara Basin than on the adjacent continental margin. However, the principal sediment components in Hole 893A are terrigenous silt

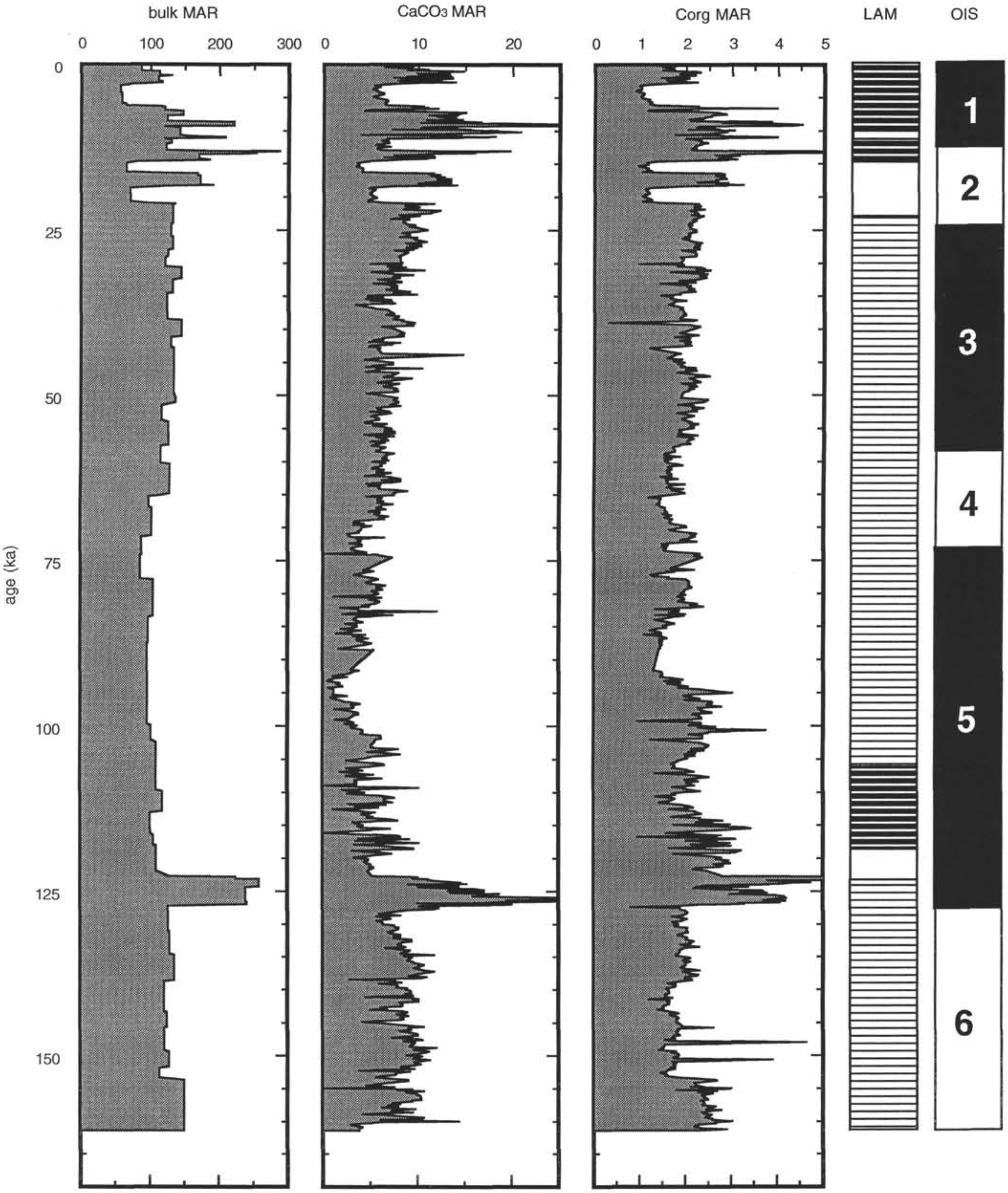

Figure 10. Bulk MAR, $CaCO_3$ MAR, and C_{org} MAR vs. age for Hole 893A. All MARs are in units of g/cm² k.y. See Figure 6 caption for explanation of far-right columns, which are plotted vs. age.

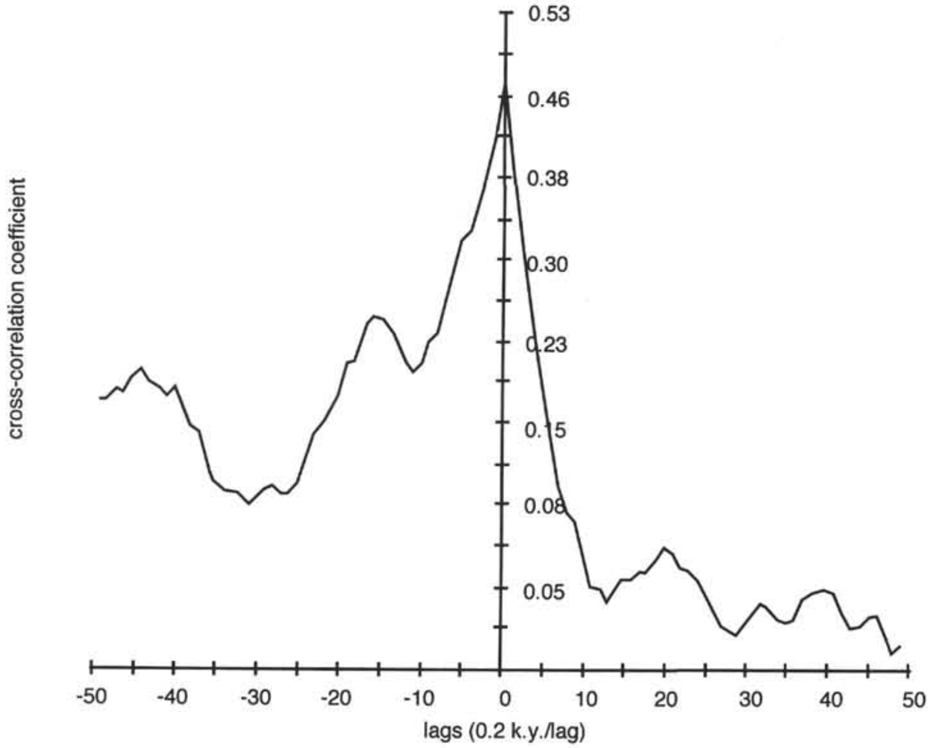

Figure 11. Cross-correlation coefficients between $CaCO_3$ MAR and C_{org} MAR over ± 10 k.y. shifts at 0.2 k.y./shift.

and clay, as shown by the extremely high bulk MARs, as well as by smear-slide estimates. Although no measurements of biogenic opal are available, smear slides rarely show even common abundances of diatoms and radiolarians, and the $CaCO_3$ fluxes are an order-of-magnitude lower than the bulk-sediment fluxes. Runoff from the Ventura and Santa Clara Rivers, along with down-slope transport from the surrounding margins of the basin must account for the extremely high total flux of material that has accumulated in the basin proper. Even though the fluxes of $CaCO_3$ and C_{org} are higher than occur along an open continental margin, the component that has accounted for most of the sediment mass in the basin is terrigenous silt and clay, not biogenic debris.

Preservation of C_{org}-rich Sediments

There has been a lively discussion in the literature about whether anoxic conditions are required to preserve C_{org}-rich sediments. Henrichs and Reeburgh (1987), Calvert (1987), Pedersen and Calvert (1990), Pedersen et al., (1992), and Calvert and Pedersen, (1992) contend that anoxia is not a prerequisite for the enhanced preservation of C_{org}; rather a high flux of C_{org} to the bottom is the requirement, regardless of the amount of dissolved oxygen in the bottom waters. Another group (Schlanger and Jenkyns, 1976; Thiede and van Andel, 1977; Demaison and Moore, 1980; Emerson and Hedges, 1988; Dean et al., 1994) contends that anoxic to suboxic conditions are required to preserve C_{org}-rich sediments. The sediments from Hole 893A bear on this discussion because they were deposited at extremely fast and relatively constant sedimentation rates (especially before about 20 ka; Fig. 8), with a relatively high flux of C_{org}, and the bottom waters were periodically anoxic. Clearly, the laminated intervals in Hole 893A represent periods of time when the bottom waters were below the level that could support benthic biological activity; presumably it was the anoxic conditions that allowed the preservation of the laminated intervals. Consequently, if anoxia is a prerequisite for the preservation of C_{org}-rich sediments, then there should be a correlation between highest values of C_{org}, or C_{org} MAR, and the presence of laminations. The lower laminated sequence has the highest average C_{org} value (2.08 wt%) but not the highest average C_{org} flux (1.95 g/cm^2

Table 2. Means (avg.), standard deviations (σ), and correlation coefficient (r) of %$CaCO_3$, %C_{org}, and mass accumulation rates for each facies of the lamination cycles.

	ULS		UIS		UNS		LLS		LIS		LNS	
	avg.	σ	avg.	σ	avg.	σ	avg.	σ	avg.	σ	avg.	σ
%$CaCO_3$	8.32	2.8	4.90	1.6	7.04	0.8	4.50	2.0	6.48	1.6	6.37	2.1
%C_{org}	1.55	0.2	1.69	0.4	1.63	0.1	2.08	0.5	1.53	0.3	1.55	0.4
r (C_{org}:$CaCO_3$)	0.19		0.22		0.06		0.44		0.04		0.02	
bulk MAR	124	49	116	20	135	50	112	18	117	22	119	26
$CaCO_3$ MAR	10.1	4.9	5.8	2.3	9.4	3.8	5.2	2.1	6.2	2.9	6.0	3.0
C_{org} MAR	1.9	0.8	1.9	0.4	2.2	0.8	1.9	0.5	2.0	0.5	2.0	0.5
r (C_{org}:$CaCO_3$ MARs)	0.63		0.26		0.94		0.16		0.23		0.36	

Notes: ULS = upper laminated sequence, UIS = upper intermittently laminated sequence, UNS = upper non-laminated sequence, LLS = lower laminated sequence, LIS = lower intermittently laminated sequence, and LNS = lower non-laminated sequence.

k.y.) (Table 2). The other facies (laminated, intermittently laminated, non-laminated) have average percent C_{org} values ≤ 1.69%, although the highest individual values of C_{org} occur in the upper and lower intermittently laminated sequences (3.70% and 3.83%, respectively). The lower non-laminated sequence and the upper laminated sequence have the lowest values of C_{org} (0.64% and 0.63%, respectively), yet the upper non-laminated sequence has the highest mean C_{org} MAR values (2.20 g/cm^2 k.y.). All other laminated facies have average C_{org} MAR values less than 2.00 g/cm^2 k.y. The highest individual C_{org} MAR values occur in the upper laminated sequence with values of 6.00 g/cm^2 k.y. whereas all other laminated facies have individual maximum values of less than 4.90 g/cm^2 k.y. Consequently, when anoxic bottom-water conditions prevailed in Santa Barbara Basin (laminated and intermittently laminated facies), the highest values of C_{org} were preserved; when the highest

flux of C_{org} occurred (upper non-laminated sequence), there was enough dissolved oxygen to allow the benthos to destroy the annual layering. During conditions when oxic conditions prevailed (non-laminated facies), the lowest percentages of C_{org} were preserved. In addition, the most striking period of C_{org} flux (OIS-5) occurred during the lower laminated and lower intermittently laminated sequences.

Paleo New Productivity

The flux of C_{org} in the deep sea and along continental margins has been used to estimate new productivity (often called paleoproductivity), a measure of the particulate flux of C_{org} from the euphotic zone (Müller and Suess, 1979; Sarnthein et al., 1987; 1988; Lyle et al., 1988; Berger et al., 1989). Many of these studies determined paleoproductivity as some function of C_{org} MAR, %C_{org}, linear sedimentation rate, and DBD. Sarnthein et al. (1988) refined the equations of Müller and Suess (1979) to estimate paleoproductivity by adding new empirical data to the regressions and including depth as a parameter. Paleoproductivity has also been modeled by Suess (1980) and, to some degree, by Martin et al (1987). All of the above studies used sediment traps to measure both the flux of C_{org} and biological productivity and developed regression equations to relate the two variables. Regardless of the equations used, all estimated productivity values are within ~50% of one another and all estimates show the same general trends. We used the data of Sarnthein et al. (1988) because it has the largest compilation of measured data.

Although we have no data to indicate the proportion of the C_{org} that was contributed by terrestrial carbon to Santa Barbara Basin, we will assume, for the sake of exploration, that the flux of C_{org} into Santa Barbara Basin had the same proportions of terrestrial C_{org} as do continental margins (data of Sarnthein et al., 1988). Using our regression of the data from Sarnthein et al. (1988) discussed in the methods section (Fig. 5), we used C_{org} MAR as a proxy for paleoproductivity in Santa Barbara Basin and generated the stratigraphy shown in Figure 12. Productivity (keeping in mind the unknown contribution from terrestrial sources) was relatively high (0.5 to 1 σ above the mean) during OIS-6, but rapidly decreased at about 152 ka and remained low until earliest OIS-5. Oxygen-isotope Stage 5e is marked by a very rapid and high rate of productivity (greater than +2 σ above the mean), but this may be the result of the suspicious interval sedimentation rate at this level. Otherwise, productivity during OIS-5 remained less than or at about the mean. Productivity remained below the mean with relatively low variability throughout OIS-4 and OIS-3, then experienced a series of large-scale (±2 σ) fluctuations of ~2 k.y. duration throughout OIS-2 and OIS-1. Interestingly, OIS-2 and OIS-1 are very similar in regard to paleoproductivity and are dissimilar to the rest of the record. This suggests that productivity in Santa Barbara Basin may not have been controlled by global climatic forcing, but rather, by more-local conditions.

The ratio of C_{org} to inorganic carbon was suggested by Berger and Keir (1984) as a measure of paleoproductivity. Inorganic carbon represents the carbon contributed by the $CaCO_3$ tests of micro- and nannofossils. In the rain-ratio model of Berger and Keir (1984), they contend that the rain of $CaCO_3$ and C_{org} across the thermocline is a function of fertility, and they suggest that depths <1000 m in low-fertility areas have C_{org}/IC values of ~2, whereas similar depths at a high-fertility area have ratios of about 10. The ratio of C_{org} to inorganic carbon in Hole 893A shows a dramatic increase of C_{org} flux that only occurred during OIS-5 (Fig. 13). The values of C_{org}/IC during mid OIS-5 approach those measured from sediment-trap samples in the high-fertility zone of the Southern Ocean (Wefer et al., 1982). At all times other than OIS-5, the C_{org}/IC ratio is virtually the same as modern values from the relatively low-fertility regions of the Sargasso Sea and Panama Basin at 1000-m water depth (Honjo, 1980). The extremely high C_{org}/IC ratios during OIS-5 in Santa Barbara Basin suggest that the flux of biogenic silica must have been very high during this time to have diluted the carbonate carbon. OIS-5e does not stand out as a high value of C_{org}/IC, as it does in values of C_{org} MAR because C_{org}/IC is independent of the suspicious interval sedimentation rate. The four pulses of C_{org} stand out as the only periods of elevated C_{org}/IC. So, regardless of whether the C_{org} is principally from terrigenous or marine sources, the percentage of C_{org} relative to the other components was higher during OIS-5 than at any other time during the past 161 k.y.

Global and Local Responses

The final tests performed on the C_{org} and $CaCO_3$ stratigraphies from Santa Barbara Basin were a series of spectral analyses to see if any periodicities occur in the records that could be correlated to Milankovitch-band global climatic forcing (Imbrie et al, 1984) or to higher-frequency local forcing. The records of percent C_{org}, percent $CaCO_3$, C_{org} MAR, $CaCO_3$ MAR, and paleoproductivity were each interpolated into a time series with a constant 200-yr time interval, providing a Nyquest frequency (maximum resolution) of 0.0025 cycle/yr (400 yr/cycle). A series of spectral windows with periods ranging from 0.4 to 50 k.y./cycle were investigated using standard spectral techniques (Blackman and Tukey, 1958; Jenkins and Watts, 1968). The only record that shows any significant spectral power is the percent C_{org} record with a well-defined peak in spectral energy at 23 k.y./cycle (Fig. 14). This is a precession periodicity, but the peak is just significant at the 80% confidence level because only four 23-k.y. peaks occur in the otherwise rather monotonous 161-k.y. record. Surprisingly, the other parameters show essentially flat and low density-power spectra well below the 80% confidence level, indicating no periodic fluctuations in the above spectral windows. The correlation of C_{org} with precession was investigated further by cross-correlation of percent C_{org} with the precession signal for 34°N (Fig. 15). There is a low, but statistically significant (at the 80% level, $r = 0.27$) cross-correlation between fluctuations of percent C_{org} and 34°N precession. Because precession is a strong modulator of insolation at 34°N, time series of insolation for the first day of each month for the past 160 k.y. were compared with the %C_{org} time series. Curiously, the strongest coherency occurs with percent C_{org} and October insolation, the month with the lowest insolation values, and there is no coherency between percent C_{org} and April insolation, the month with the highest insolation values (Fig. 16). We have no explanation for this correlation, but we remind the reader of the suspicious sedimentation rates around 127 ka that may have contributed to this coherency.

Speculations

So, why did Santa Barbara Basin not record global climatic forcing in the records of percent $CaCO_3$, mass accumulation rates, or paleoproductivity? Why does percent C_{org} have a precessional periodicity but not C_{org} MAR and paleoproductivity, proxies calculated from percent C_{org}? Pisias (1978) found that Holocene radiolaria

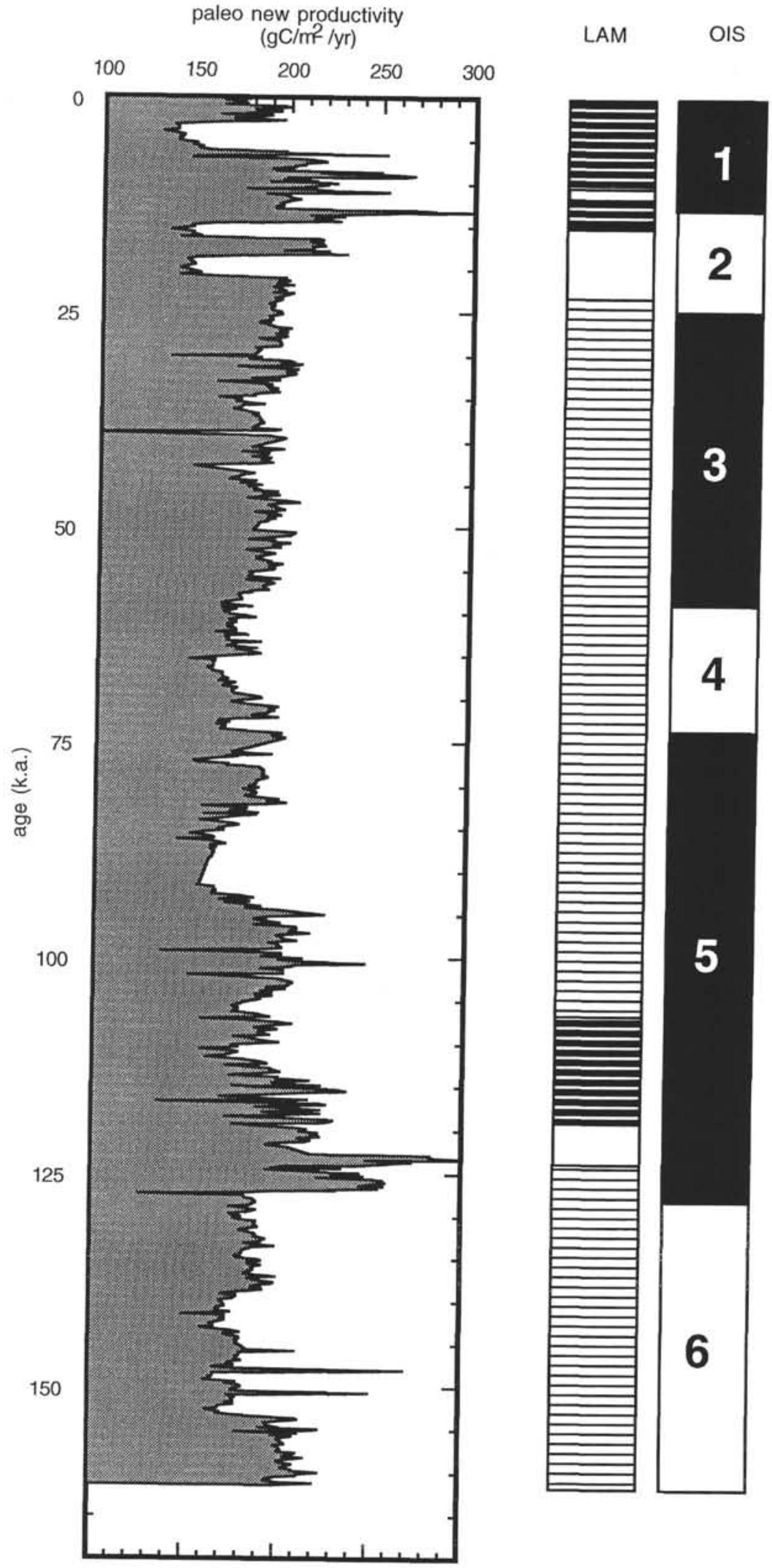

Figure 12. Paleoproductivity (using regression of data from Sarnthein et al., 1988) vs. age for Hole 893A. See text for discussion of paleoproductivity. See Figure 6 caption for explanation of far-right columns.

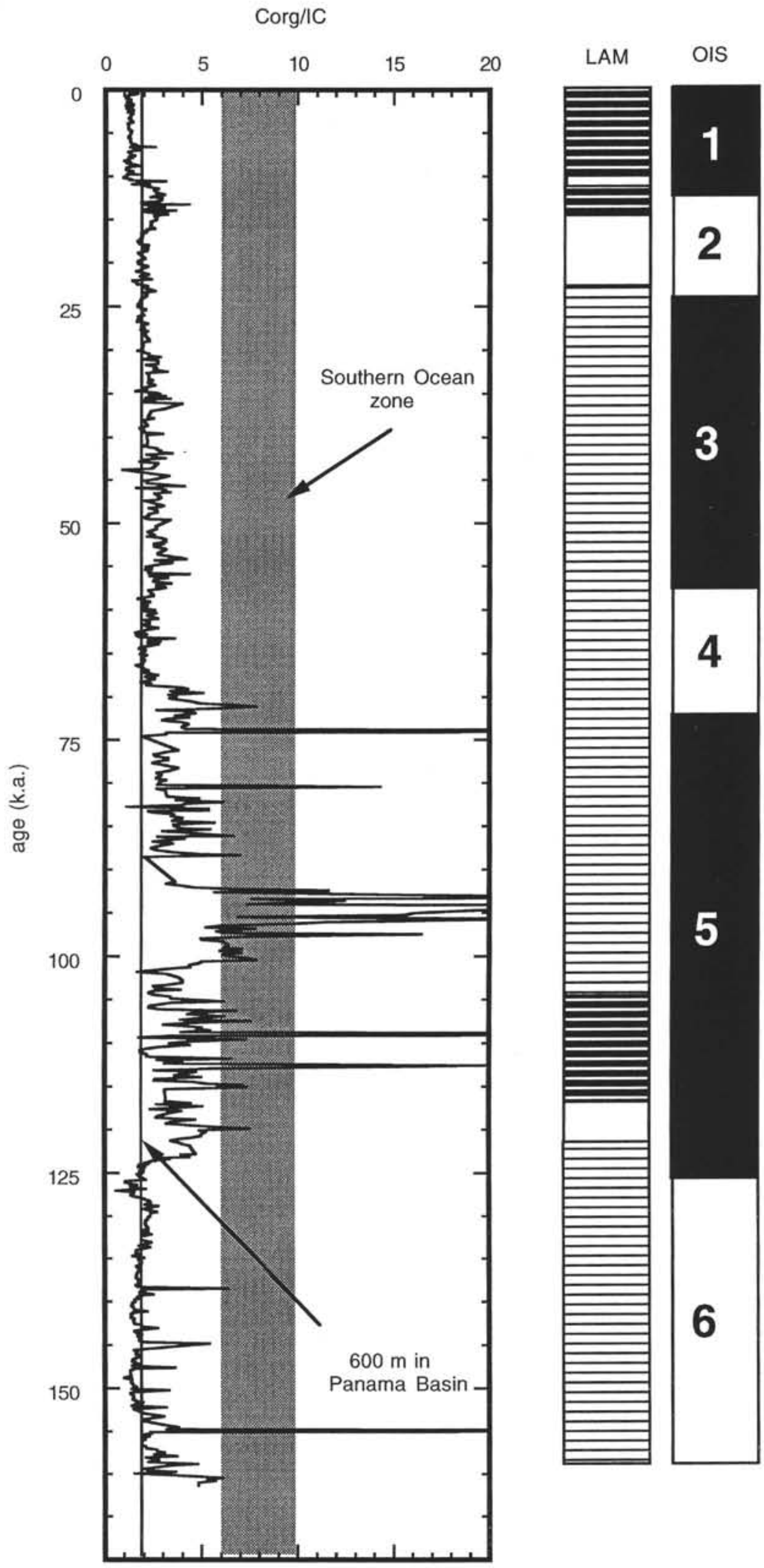

Figure 13. C_{org}/IC, an alternate proxy for paleoproductivity (after Berger and Keir, 1984) vs. age for Hole 893A. Compare with Figure 12.

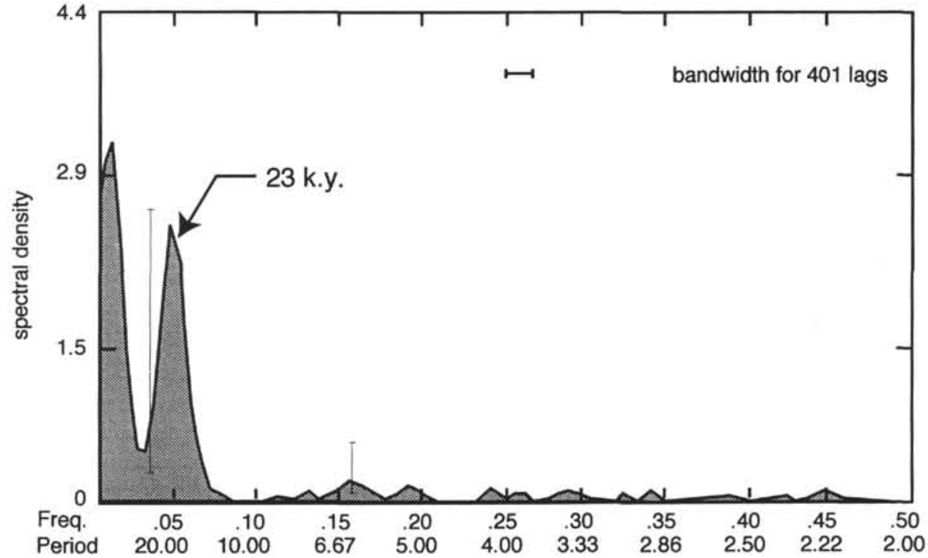

Figure 14. Power spectrum for C_{org} with a spectral window of 2 to 40 k.y./cycle. The analysis used 845 samples, 401 lags, and was calculated with a confidence interval (vertical bar) of 80%. The only peak occurs at 23 k.y., a precessional period, but is just significant at the 80% confidence level.

from a piston core from Santa Barbara Basin could be interpreted to reflect changes in the California Current, a current system that fluctuated with changing hemispheric atmospheric conditions (Pisias, 1978; Gardner and Hemphill-Haley, 1986; Anderson et al., 1990). Pollen records from both a piston core from Santa Barbara Basin (Heusser, 1978) and from Hole 893A (Heusser, 1994; Heusser, this volume) show that the local climates alternated between moist, cool conditions and a dry, warm environment. Therefore, changes *did* occur in the local environment of Santa Barbara Channel. But why are the sedimentation rates so constant, especially prior to 20 ka, in light of conditions that changed from wet to dry, etc. And why are there no responses in C_{org}, $CaCO_3$, or productivity to the undoubtedly larger changes that occurred from glacial to interglacial conditions?

One obvious answer might be that percent $CaCO_3$, fluxes, and productivity in Santa Barbara Basin were either periodically sensitive to local changes or were *only* sensitive to local changes. The study of radiolarian faunas in Santa Barbara Basin (Pisias, 1978) may provide a clue. The maximum variance in the modern radiolarian assemblages explained by a California Current factor is only 60%. The modern radiolarian assemblage in Santa Barbara Basin is a mixture of assemblages, some representative of waters to the south, some from waters to the west, and some introduced via the California Current from the north. Modern Santa Barbara Basin radiolarian assemblages do not replicate modern California Current radiolarian assemblages. The modern high eustatic sea level allows the Southern California Counter Current to transport water from the south and west through Santa Barbara Channel and over Santa Barbara Basin. However, during eustatic low sea levels, this cyclonic circulation must have been restricted (Fig. 17), and it is questionable if any significant flow occurred through the narrow (ca. 2 km) and shallow (330 m) Santa Barbara Channel. For instance, eustatic sea level was at –120 m from 22 ka to ~17 ka, was at –86 m at 12 ka, and was still at –60 m at 10 ka (Fairbanks, 1989); similar lowerings occurred during OIS-4 and OIS-6, and OIS-3 had sea levels at about ~ –40 m (Bard et al., 1990). Restricted flow would in effect make Santa Barbara Basin a back-water cul-de-sac, while the main, southward-flowing, California Current essentially bypassed the basin (Fig. 17). The extended periods of lower sea levels may have isolated Santa Barbara Basin from the main California Current by restricting the cross-sectional area of the western sill so that little or no nutrient-rich surface and near-surface waters were able to continuously enter the basin. The eastern sill may have been so severely restricted by eustatic lower sea levels that the cyclonic gyre of the California Counter Current may have been shifted to the south, isolating Santa Barbara Basin from the general circulation. Consequently, when eustatic sea level was low, the basin may have been isolated and $CaCO_3$, C_{org}, and productivity only responded to local forcing during these times (i.e., OIS-6, -4, -3, and -2). When eustatic sea level was above some threshold level, the western entrance to Santa Barbara Basin may have been widened enough to allow the import of nutrient-rich California Current water into the basin. These conditions may have existed only during OIS-5 and OIS-1.

An alternate explanation might be that during glacial periods (OIS-6, OIS-4, parts of OIS-3, and OIS-2, and possibly the Younger Dryas) sea-surface temperatures in Santa Barbara Basin cooled, thereby reducing the vertical stratification in the water column. However, it is difficult to understand how a reduced vertical stratification would isolate Santa Barbara Basin from the main California Current during these times. An actual restriction in the communication of Santa Barbara Basin with the California Current seems the most reasonable explanation of the lack of response to global forcing.

However, there is evidence that some parameters in Santa Barbara Basin responded to at least a hemisphere-scale forcing. The only published record of data from another long core influenced by the California Current is that from Deep Sea Drilling Project (DSDP) Site 480, a 150-m-long hydraulic piston core from 655-m water depth in the Guaymas Basin, Gulf of California (Curray, Moore, et al., 1982). Although it is problematic whether or not Pacific Intermediate Water (PIW) flows directly into Santa Barbara Basin because of its shallow sill depth, Site 480 in Guaymas Basin is clearly bathed by PIW. Keigwin and Jones (1990) published an AMS ^{14}C-dated age model for the last 22 k.y. of DSDP Site 480, together with percent $CaCO_3$, percent C_{org}, and an interpretation of the laminated sequences. The sedimentation rates at Site 480 are similar to those at Hole 893A, and the Site 480 laminated sequence for the last 22 k.y. is remarkably similar to that of Hole 893A, even to the non-laminated interval that coincides with a Younger Dryas-aged event (Fig. 18). We interpret this remarkable correlation over a distance of ~2500 km to ultimately be the result of the dissolved-oxygen content of PIW and the water that immediately overlies it. Periods of laminated sediment in Santa Bar-

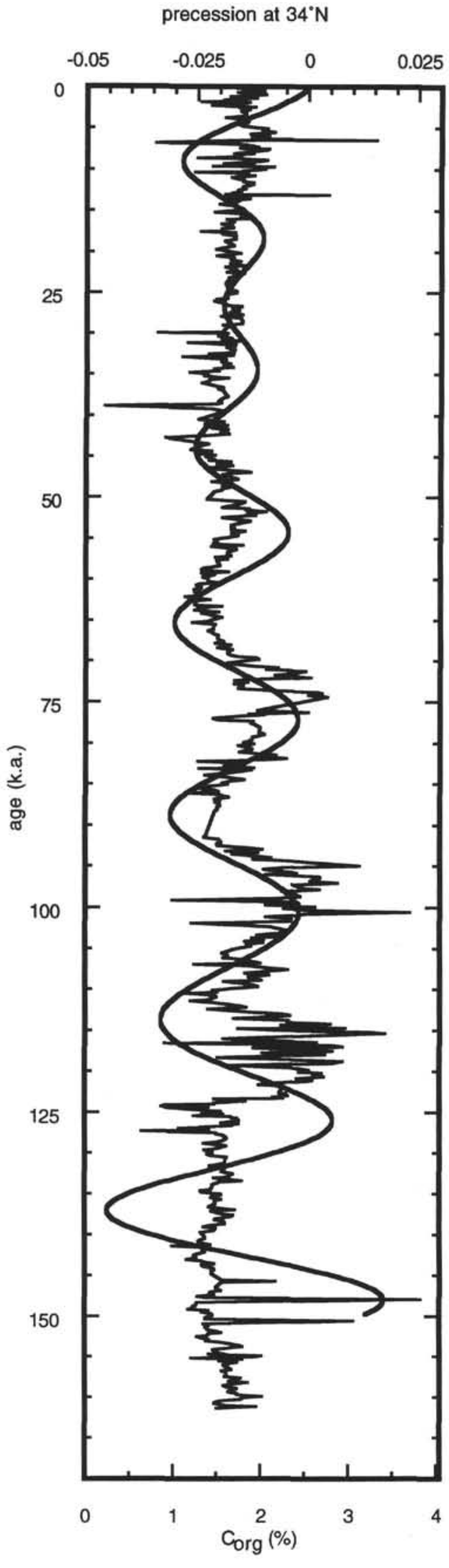

Figure 15. Precession at 34°N for the past 150 k.y. plotted over C_{org} percentages for Hole 893A. Cross-correlation coefficient between the two parameters = 0.27.

bara Basin (~15 to 13 ka and 11 ka to present) represent periods when either the flow of intermediate water into the basin was weak or upwelling along the open margin of California was strong enough to deplete the dissolved oxygen to levels below that required for benthic respiration. Either of these conditions could have rendered the shallow subsurface water that entered Santa Barbara Basin suboxic to anoxic. Sequences of bioturbated (non-laminated) sediment in Santa Barbara Basin must represent periods when its bottom waters were more oxygenated than today, so that benthic respiration did not deplete the dissolved oxygen. Alternately, additional PIW could have been periodically generated at some locality different from today's northwestern Pacific site (Reid, 1965; Talley, 1991), such as the Alaska Gyre (Van Scoy et al., 1991) which would have increased the volume of PIW and possibly decreased its depth of influence. The addition of a source of well-oxygenated water injected into PIW closer to the western margin of North America may have provided enough additional oxygen to maintain PIW at oxic levels throughout its passage along the California margins and through the Gulf of California. Piston cores along the open central California margin do not have laminations in the upper 25 k.y. of the section, but many do have laminated intervals in sediments older than 25 ka (Gardner and Hemphill-Haley, 1986; Anderson et al., 1989; Gardner, et al., 1992; Hemphill-Haley and Gardner, 1994). The lack of correlation of cores from the open margin to Santa Barbara Basin may reflect the periodic addition of another source of PIW together with only sporadic ventilation of Santa Barbara Basin by pulses of oxygenated water breaching over the western sill and the quick biologic reduction of the imported oxygen (Sholkovitz and Gieskes, 1971; Reimers et al., 1990). The open California margin has no restrictions to the flow of PIW so that oxygen is being continuously supplied by the flow. Possibly it is the central California upwelling that reduces oxygen, but not to anoxia levels, in waters directly above PIW prior to them reaching Santa Barbara Basin. Additional depletion of dissolved oxygen by biological consumption along the Baja California margin may ensure suboxic to anoxic PIW in the Guaymas Basin. Ventilation events, as occurred during OIS-5, OIS-2, and the last deglaciation, affected all four areas (central California margin, Santa Barbara Basin, Baja California margin, Guaymas Basin margin). Profiles of percent $CaCO_3$ or percent C_{org} from Site 480 do not correlate with those from Hole 893A (Fig. 18), suggesting that the responses of $CaCO_3$ and C_{org} are results of local conditions, such as basin isolation, local productivity, runoff, erosion rates, surface geology, etc.

CONCLUSIONS

Hole 893A has been analyzed at a sampling interval of 100 to 150 yr/sample for the entire 161 k.y. record. Stratigraphies of $CaCO_3$ and total C_{org} (terrigenous + marine C_{org}) show variations over the past 161 k.y. but only within rather narrow limits of ~2% to 14% $CaCO_3$. Calcium carbonate does not correlate with glacial-interglacial cycles nor with the presence or absence of laminated sediment, and has a low variability during all periods but early OIS-1. Total C_{org} percentages varies much less than percent $CaCO_3$ does, but large variations in C_{org} occur in OIS-5 and early OIS-3. Four periods of high C_{org} and high variability occur with a 23-k.y./cycle periodicity and statistical coherency with precession and 34°N insolation, suggesting astronomical forcing. However, neither C_{org} or $CaCO_3$ show any periodical variations, other than the 23 k.y./cycle in percent C_{org}, in the frequency band of 400 to 40,000 yr. An intriguing observation is that the one lamination cycle recovered at Hole 893A is 100 k.y. in duration, suggesting a possible eccentricity forcing to the ventilation of Santa Barbara Basin. However, further speculation on this correlation must await much longer records.

Mass accumulation rates of bulk sediment, $CaCO_3$, and C_{org} also show no correlations with glacial-interglacial cycles or with lamination cycles. Mass accumulation rates of bulk sediment, $CaCO_3$, and C_{org} are all an order-of-magnitude higher than occur on the adjacent

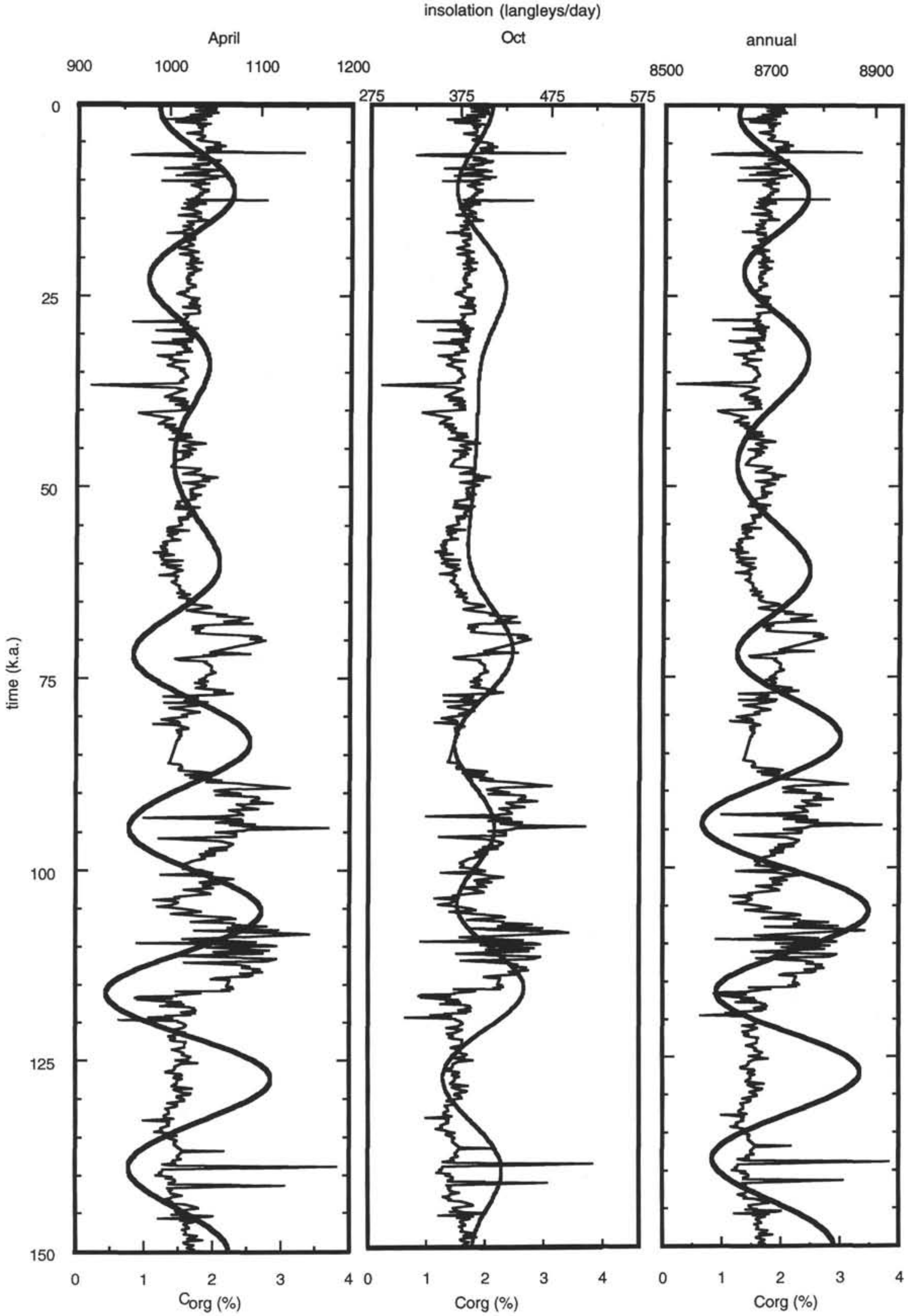

Figure 16. C_{org} percentages for Hole 893A overlain with a 150-k.y. record of insolation for 34°N on April 1, October 1, and total annual insolation at 34°N. Insolation in langleys/day. Note the good correlation for October, but poor correlations for April and annual insolations.

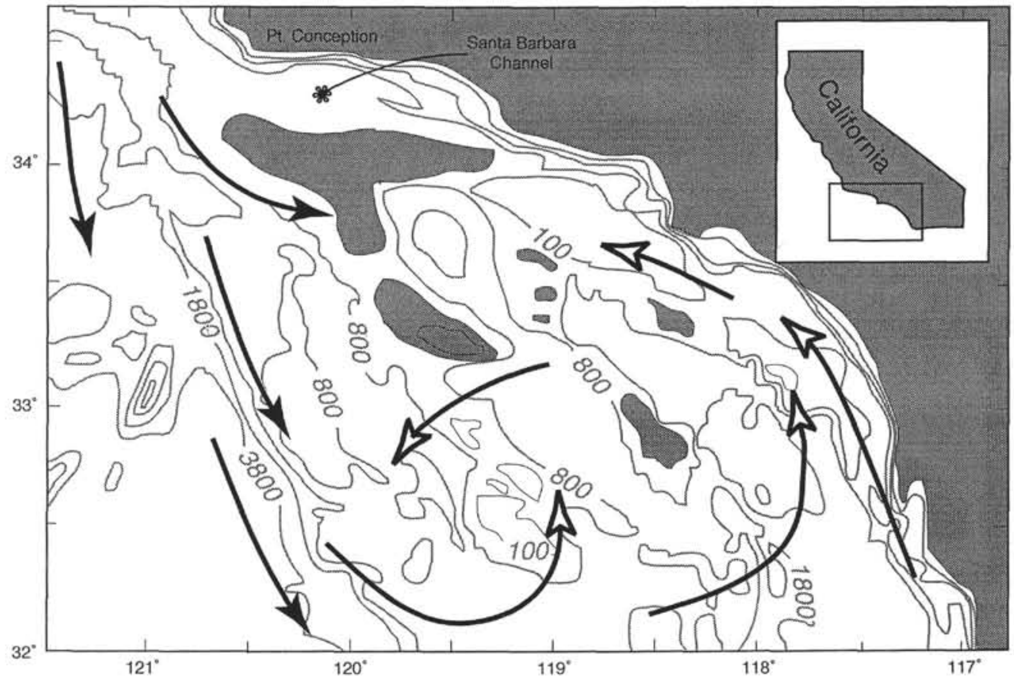

Figure 17. Hypothesized surface circulation during periods of low eustatic sea levels. Compare with Figure 3 and notice the lack of California Current flow into Santa Barbara Channel and the southward shift of the cyclonic California Counter Current (modified from Hickey, 1992). Bathymetry in meters.

open margin. The fact that the percentages of $CaCO_3$ and C_{org} of Santa Barbara Basin are similar to those from the adjacent open margin indicates that Santa Barbara Basin acted as an amplifier of sediment flux, producing the extreme sedimentation rates.

Paleoproductivity is difficult to evaluate from our measurements of total C_{org} because no organic geochemistry is available to determine the contribution from terrestrial vs. marine C_{org}. However, a comparison of results from two different methods to determine paleoproductivity suggests that productivity was greatly enhanced during OIS-5 and early OIS-3 relative to the rest of the record.

Sea level has played an important role in determining what Santa Barbara Basin sediment responds to.During eustatic high sea levels, such as today, nutrient-rich California Current water is directly advected into Santa Barbara Channel with additional water being supplied by the cyclonic California Counter Current. However, when eustatic sea level was lower than today, by some threshold amount, the narrow sills of Santa Barbara Basin were restricted enough to exclude continuous direct advection, and the emergent island platform of the Santa Rosa-Cortez Ridge deflected the California Counter Current south of Santa Barbara Basin. There is some suggestion that the threshold depth may be ca. –40 m.

The bathymetric restrictions apparently only affected the wind-driven circulation in Santa Barbara Channel. The striking similarity in the lamination cycles for the last 22 k.y. from Guaymas Basin and Santa Barbara Basin suggests that Pacific Intermediate Water may have shoaled or at least affected overlying intermediate-depth waters. These waters imported more dissolved oxygen into the eastern Pacific margin during OIS-2 but became depleted (and possibly sank) about 15 ka and remained so for the entire Holocene, with the exception of a short-duration ventilation event, correlated in time with the Younger Dryas (12 to 13 ka, calendar years) that is recorded in sediments from both the Guaymas Basin and Santa Barbara Basin. The similarity in the lamination cycles of the two basins suggests a hemispheric-scale atmospheric forcing that may reflect a regulation of the dissolved-oxygen content of Pacific Intermediate Water either with a periodic additional source or an increase in volume and/or advection speed during OIS-2.

ACKNOWLEDGMENTS

We appreciate the many discussions and free flow of ideas we have had with several colleagues, especially Walt Dean, Rick Behl, Frank Rack, Eileen Hemphill-Haley, Linda Heusser, Nick Pisias, and Jim Kennett, over the course of this manuscript. We wish to thank Walt Dean, Doug Hammon, and John Compton for thoughtful and very constructive reviews of earlier versions of this manuscript. Although we disagree with some of our colleagues on some aspects of the diagenesis of C_{org}, the subject has given rise to a lively and entertaining debate.

REFERENCES

Anderson, R.Y., Gardner, J.V., and Hemphill-Haley, E., 1989. Variability of the late Pleistocene-early Holocene oxygen-minimum zone off northern California. *In* Peterson, D.H. (Ed.), *Aspects of Climate Variability in the Pacific and Western Americas.* Geophys. Monogr., Am. Geophys. Union, 55:75–84.

Anderson, R.Y., Linsley, B.K., and Gardner, J.V., 1990. Expression of seasonal and ENSO forcing in climatic variability at lower than ENSO frequencies: evidence from Pleistocene marine varves off California. *Palaeogeogr., Palaeoclimatol., Palaeoecol.,* 78:287–300.

Arrhenius, G., 1952. Sediment cores from the East Pacific. *In* Pettersson, H. (Ed.), *Rep. Swed. Deep-Sea Exped., 1947–1948,* 5:189–201.

Bard, E., Hamelin, B., and Fairbanks, R.G., 1990. U-Th ages obtained by mass spectrometry in corals from Barbados: sea level during the past 130,000 years. *Nature,* 346:456–458.

Berger, W.H., and Keir, R.S., 1984. Glacial-Holocene changes in atmospheric CO_2 and the deep-sea record. *In* Hansen, J.E., and Takahashi, T. (Eds.), *Climate Processes and Climate Sensitivity.* Geophys. Monogr., Maurice Ewing Ser. 5, Am. Geophys. Union, 29:337–351.

Berger, W.H., Smetacek, V.S., and Wefer, G. (Eds.), 1989. *Productivity of the Ocean: Present and Past:* New York (Wiley).

Berner, R.A., 1982. Burial of organic carbon and pyrite sulfur in the modern ocean: its geochemical and environmental significance. *Am. J. Sci.,* 282:451–473.

Blackman, R.B., and Tukey, J.H., 1958. *The Measurement of Power Spectra From the Point of View of Communication Engineering:* Mineok, NY (Dover).

Calvert, S.E., 1987. Oceanographic controls on the accumulation of organic matter in marine sediments. *In* Brooks, J., and Fleet, A.J. (Eds.), *Marine Petroleum Source Rocks.* Geol. Soc. Spec. Publ. London, 26:137–151.

Calvert, S.E., and Pedersen, T.F., 1992. Organic carbon accumulation and preservation in marine sediments: how important is anoxia? *In* Whelan, J.K., and Farrington, J.W. (Eds.), *Productivity, Accumulation and Preservation of Organic Matter in Recent and Ancient Sediments:* New York (Columbia Univ. Press).

Curray, J.R., Moore, D.G., et al., 1982. *Init. Repts. DSDP,* 64 (Pts. 1 and 2): Washington (U.S. Govt. Printing Office).

Dean, W.E., Gardner, J.V., and Anderson, R.Y., 1994. Geochemical evidence for enhanced preservation of organic matter in the oxygen minimum zone of the continental margin of northern California during the late Pleistocene. *Paleoceanography,* 9:47–61.

Demaison, G.J., and Moore, G.T., 1980. Anoxic environments and oil source bed genesis. *AAPG Bull.,* 64:1179–1209.

Drake, D.E., Kolpack, R.L., and Fischer, P.J., 1972. Sediment transport on the Santa Barbara-Oxnard shelf, Santa Barbara Channel, California. *In* Swift, D.J.P., Duane, D.B., and Pilkey, O.H. (Eds.), *Shelf Sediment Transport: Process and Pattern:* Stroudsburg, PA (Dowden, Hutchinson, and Ross), 307–331.

Emerson, S., 1985. Organic carbon preservation in marine sediments. *In* Sundquist, E.T., and Broecker, W.S. (Eds.), *The Carbon Cycle and Atmospheric CO_2: Natural Variations Archean to Present:* Geophys. Monogr., Am. Geophys. Union, 32:78–87.

Emerson, S., Fischer, K., Reimers, C., and Heggie, D., 1985. Organic carbon dynamics and preservation in deep-sea sediments. *Deep-Sea Res. Part A,* 32:1–21.

Emerson, S., and Hedges, J.I., 1988. Processes controlling the organic carbon content of open ocean sediments. *Paleoceanography,* 3:621–634.

Emery, K.O., 1960. *The Sea Off Southern California: A Modern Habitat of Petroleum:* New York (Wiley).

Emery, K.O., and Hülsemann, J., 1962. The relationships of sediments, life and water in a marine basin. *Deep-Sea Res. Part A,* 8:165–180.

Engleman, E.E., Jackson, L.L., and Norton, D.R., 1985. Determination of carbonate carbon in geological materials by coulometric titration. *Chem. Geol.,* 53:125–128.

Fairbanks, R.G., 1989. A 17,000-year glacio-eustatic sea level record: influence of glacial melting rates on the Younger Dryas event and deep-ocean circulation. *Nature,* 342:637–642.

Fleischer, P., 1972. Mineralogy and sedimentation history, Santa Barbara Basin, California. *J. Sediment. Petrol.,* 42:49–58.

Gardner, J.V., Dean, W.E., and Kayen, R., 1992. USGS Cruise F2-92, central and southern California margin. *Open-File Rep.—U.S. Geol. Surv.,* 92–342.

Gardner, J.V., and Hemphill-Haley, E., 1986. Evidence for a stronger oxygen-minimum zone off central California during late Pleistocene to early Holocene. *Geology,* 14:691–694.

Heath, G.R., Moore, T.C., Jr., and Dauphin, J.P., 1977. Organic carbon in deep-sea sediments. *In* Andersen, N.R., and Malahoff, A. (Eds.), *The Fate of Fossil Fuel CO_2 in the Oceans:* New York (Plenum), 605–625.

Hemphill-Haley, E., and Gardner, J.V., 1994. Revised ages for laminated-sediment intervals and a Holocene-marker diatom from the northern California continental slope. *Quat. Res.,* 41:131–135.

Henrichs, S.M., and Reeburgh, W.S., 1987. Anaerobic mineralization of marine sediment organic matter: rates and the role of anaerobic processes in the oceanic carbon economy. *J. Geomicrobiol.,* 5:191–237.

Heusser, L., 1978. Pollen in Santa Barbara Basin, California: a 12,000 year record. *Geol. Soc. Am. Bull.,* 89:673–678.

————, 1994. Continuous pollen/paleoclimate records from the last glacial cycle: ODP Hole 893A, Santa Barbara Basin. *Eos,* 75 (Suppl.):201.

Hickey, B.M., 1979. The California Current System—hypotheses and facts. *Prog. Oceanogr.,* 8:191–279.

————, 1992. Circulation over the Santa Monica-San Pedro basin and shelf. *Prog. Oceanogr.,* 30:37–115.

Honjo, S., 1980. Material fluxes and modes of sedimentation in the mesopelagic and bathypelagic zones. *J. Mar. Res.,* 38:53–97.

Hülsemann, J., and Emery, K.O., 1961. Stratification in recent sediments of Santa Barbara Basin as controlled by organisms and water character. *J. Geol.,* 69:279–290.

Imbrie, J., Hays, J.D., Martinson, D.G., McIntyre, A., Mix, A.C., Morley, J.J., Pisias, N.G., Prell, W.L., and Shackleton, N.J., 1984. The orbital theory of Pleistocene climate: support from a revised chronology of the marine $\delta^{18}O$ record. *In* Berger, A., Imbrie, J., Hays, J., Kukla, G., and Saltzman, B. (Eds.), *Milankovitch and Climate* (Pt. 1): Dordrecht (D. Reidel), 269–305.

Jenkins, G.M., and Watts, D.G., 1968. *Spectral Analysis and Its Applications:* Oakland (Holden Day).

Keigwin, L.D., and Jones, G.A., 1990. Deglacial climatic oscillations in the Gulf of California. *Paleoceanography,* 5:1009–1023.

Lyle, M., Murray, D.W., Finney, B.P., Dymond, J., Robbins, J.M., and Brooksforce, K., 1988. The record of Late Pleistocene biogenic sedimentation in the eastern tropical Pacific Ocean. *Paleoceanography,* 3:39–59.

Lyle, M., Zahn, R., Prahl, F., Dymond, J., Collier, R., Pisias, N., and Suess, E., 1992. Paleoproductivity and carbon burial across the California Current: the Multitracers Transect, 42°N. *Paleoceanography,* 7:251–272.

Martin, J.H., Knauer, G.A., Karl, D.M., and Broenkow, W.W., 1987. VETEX: carbon cycling in the northeast Pacific. *Deep-Sea Res.,* 34:267–285.

Martin, W.R., and Bender, M.L., 1988. The variability of benthic fluxes and sedimentary remineralization rates in response to seasonally variable organic carbon rain rates in the deep sea: a modeling study. *Am. J. Sci.,* 288:541–574.

Martinson, D.G., Pisias, N.G., Hays, J.D., Imbrie, J., Moore, T.C., Jr., and Shackleton, N.J., 1987. Age dating and the orbital theory of the ice ages: development of a high-resolution 0 to 300,000-year chronostratigraphy. *Quat. Res.,* 27:1–29.

Middelburg, J.J., 1989. A simple rate model for organic matter decomposition in marine sediments. *Geochim. Cosmochim. Acta,* 53:1577–1581.

Müller, P.J., and Suess, E., 1979. Productivity, sedimentation rate, and sedimentary organic matter in the oceans, I. Organic carbon preservation. *Deep-Sea Res. Part A,* 26:1347–1362.

Pedersen, T.F., and Calvert, S.E., 1990. Anoxia vs. productivity: what controls the formation of organic-carbon-rich sediments and sedimentary rocks? *AAPG Bull.,* 70:318–329.

Pedersen, T.F., Shimmield, G.B., and Price, N.B., 1992. Lack of enhanced preservation of organic matter in sediments under the oxygen minimum on the Oman Margin. *Geochim. Cosmochim. Acta,* 56:545–551.

Pisias, N.G., 1978. Paleoceanography of the Santa Barbara Basin during the last 8000 years. *Quat. Res.,* 10:366–384.

Reid, J.L., 1965. *Intermediate Waters of the Pacific Ocean:* Baltimore (Johns Hopkins Press).

Reimers, C.E., Lange, C.B., Tabak, M., and Bernhard, J.M., 1990. Seasonal spillover and varve formation in the Santa Barbara Basin, California. *Limnol. Oceanogr.,* 35:1577–1585.

Sarnthein, M., Winn, K., Duplessy, J.-C., and Fontugne, M.R., 1988. Global variations of surface ocean productivity in low and mid latitudes: influence on CO_2 reservoirs of the deep ocean and atmosphere during the last 21,000 years. *Paleoceanography,* 3:361–399.

Sarnthein, M., Winn, K., and Zahn, R., 1987. Paleoproductivity of oceanic upwelling and the effect on atmospheric CO_2 and climatic change during glaciation times. *In* Berger, W.H., and Labeyrie, L.D. (Eds.), *Abrupt Climatic Change: Evidence and Implications:* Dordrecht (D. Reidel), 311–337.

Schlanger, S.O., and Jenkyns, H.C., 1976. Cretaceous oceanic anoxic events: causes and consequences.*Geol. Mijnbouw,* 55:179–184.

Sholkovitz, E.R., and Gieskes, J.M., 1971. A physical-chemical study of the flushing of the Santa Barbara Basin. *Limnol. Oceanogr.,* 16:479–489.

Soutar, A., and Crill, P.A., 1977. Sedimentation and climatic patterns in the Santa Barbara Basin during the 19th and 20th centuries. *Geol. Soc. Am. Bull.,* 88:1161–1172.

Soutar, A., Kling, S.A., Crill, P.A., Duffrin, E., and Bruland, K.W., 1977. Monitoring the marine environment through sedimentation. *Nature,* 266:136–139.

Suess, E., 1980. Particulate organic carbon flux in the oceans: surface productivity and oxygen utilization. *Nature,* 288:260–263.

Talley, L.D., 1991. An Okhotsk Sea water anomaly: implications for ventilation in the North Pacific. *Deep-Sea Res.,* 38 (Suppl.):171–190.

Thiede, J., and van Andel, T.J., 1977. The paleoenvironment of anaerobic sediments in the late Mesozoic South Atlantic Ocean. *Earth Planet. Sci. Lett.,* 33:301–309.

Thornton, S.E., 1984. Basin model for hemipelagic sedimentation in a tectonically active continental margin: Santa Barbara Basin, California continental borderland. *In* Stow, D.A.V., and Piper, D.J.W. (Eds.), *Fine-grained Sediments: Deep-water Processes and Facies.* Geol. Soc. Spec. Publ. London, 15:377–394.

———, 1986. Origin of mass flow sedimentary structures in hemipelagic basin deposits: Santa Barbara Basin, California Borderland. *Geo-Mar. Lett.*, 6:15–19.

Van Scoy, K.A., Olson, D.B., and Fine, R.A., 1991. Ventilation of North Pacific Intermediate Waters: the role of the Alaskan Gyre. *J. Geophys. Res.*, 96:16801–16810.

Wefer, G., Suess, E., Balzer, W., Liebezeit, G., Müller, P.J., Ungerer, C.A., and Zenk, W., 1982. Fluxes of biogenic components from sediment trap deployment in circumpolar waters of the Drake Passage. *Nature*, 299:145–147.

Date of initial receipt: 11 July 1994
Date of acceptance: 13 February 1995
Ms 146SR-290

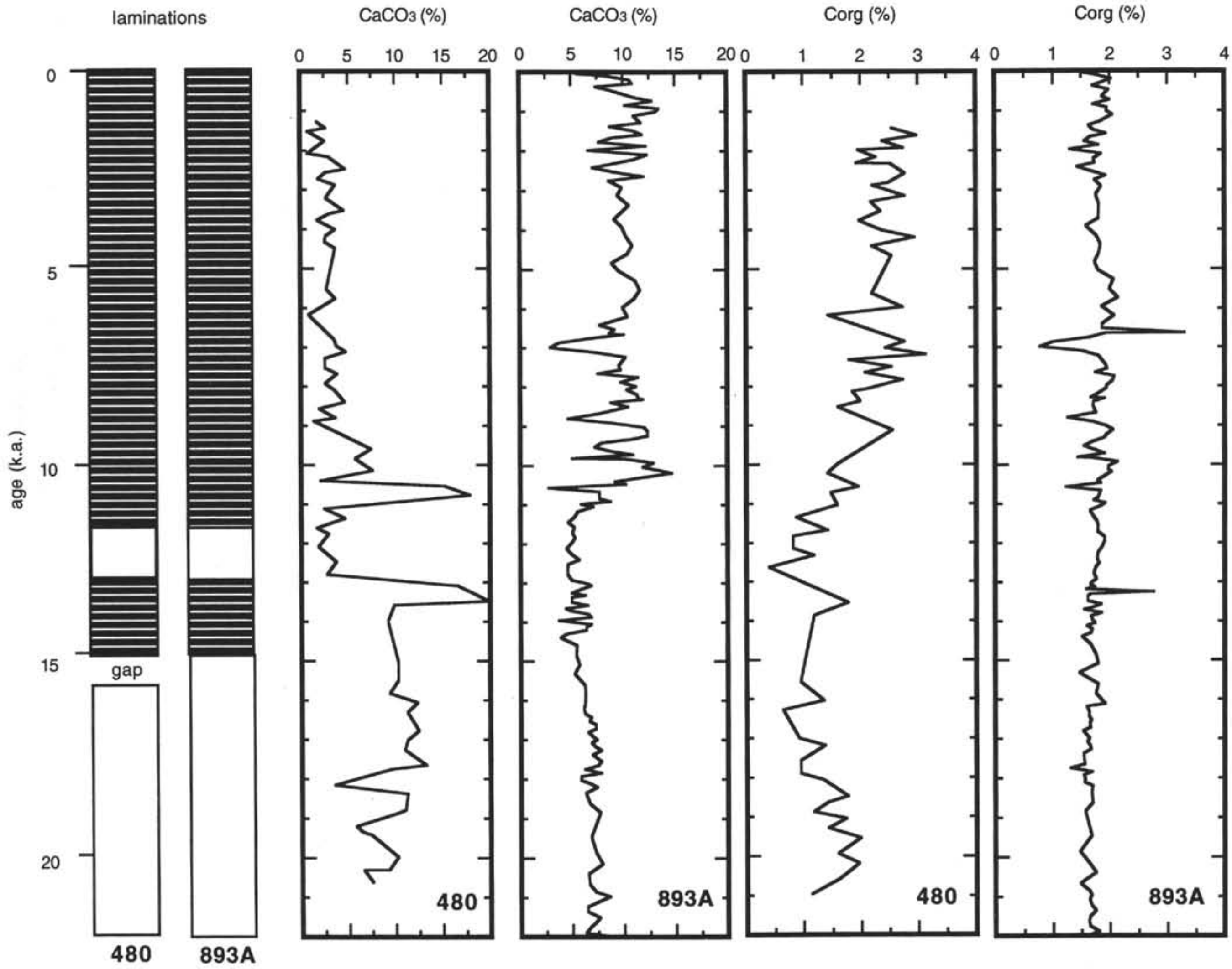

Figure 18. Comparison of lamination cycles (dark bars = laminated intervals, white areas = bioturbated intervals), percent $CaCO_3$, and percent C_{org} from Hole 893A (Santa Barbara Basin) and Site 480 (Guaymas Basin). Ages in calendar years (Site 480 data from Keigwin and Jones, 1990).

APPENDIX
Example of Analytical $CaCO_3$ and C_{org} Data from Santa Barbara Basin, Hole 893A

Core, section, interval (cm)	Uncorrected depth (m)	Corrected depth (m)	Age (ka)	% Total carbon	% Inorganic carbon	% Organic carbon	% $CaCO_3$
146-893A-							
1H-1, 7-8	0.07	0.07	0.032	3.38	0.68	2.7	5.64
1H-1, 21–21	0.21	0.21	0.101	4.04	1.01	3.03	8.38
1H-1, 40–41	0.4	0.40	0.2	4.78	1.28	3.5	10.62
1H-1, 60–61	0.6	0.60	0.307	4.49	1.31	3.18	10.87
1H-1, 80–81	0.8	0.80	0.417	3.79	0.89	2.9	7.39
1H-1, 100–101	1	1.00	0.528	4.43	1.07	3.36	8.88
1H-1, 120–121	1.2	1.20	0.64	2.41	0.52	1.89	4.32
1H-1, 140–141	1.4	1.40	0.754	4.48	1.35	3.13	11.21
1H-2, 10–11	1.6	1.58	0.857	4.87	1.54	3.33	12.78
1H-2, 31–32	1.81	1.79	0.978	4.07	1.23	2.84	10.21
1H-2, 49–50	1.99	1.97	1.082	4.84	1.62	3.22	13.45
1H-2, 69–70	2.19	2.17	1.199	4.77	1.58	3.19	13.11
1H-2, 90–91	2.4	2.38	1.322	4.66	1.33	3.33	11.04
1H-2, 109–110	2.59	2.57	1.434	3.07	0.83	2.24	6.89
1H-2, 129–130	2.79	2.77	1.552	4.37	1.41	2.96	11.7
1H-2, 149–150	2.99	2.97	1.671	3.67	1.05	2.62	8.72
1H-3, 20–21	3.22	3.19	1.802	4.06	1.33	2.73	11.04
1H-3, 40–41	3.42	3.39	1.922	4.49	1.42	3.07	11.79
1H-3, 60–61	3.62	3.59	2.042	3.7	1.07	2.63	8.88
1H-3, 80–81	3.82	3.79	2.163	3.39	0.93	2.46	7.72
1H-3, 99–100	4.01	3.98	2.278	4.29	1.47	2.82	12.2
1H-3, 119–120	4.21	4.18	2.4	2.82	0.8	2.02	6.64
1H-3, 139–140	4.41	4.38	2.521	4.34	1.48	2.86	12.28
1H-4, 10–11	4.62	4.60	2.656	3.96	1.32	2.64	10.96
1H-4, 31–32	4.83	4.81	2.784	3.72	1.08	2.64	8.96
1H-4, 49–50	5.01	4.99	2.895	3.01	0.85	2.16	7.06
1H-4, 71–72	5.23	5.21	3.03	3.7	1.14	2.56	9.46
1H-4, 90–91	5.42	5.40	3.147	4.31	1.44	2.87	11.95
1H-4, 109–110	5.61	5.59	3.264	3.62	1.04	2.58	8.63
1H-4, 130–131	5.82	5.78	3.382	3.92	1.19	2.73	9.88
1H-4, 149–150	6.01	5.97	3.5	3.69	1.14	2.55	9.46
1H-5, 20–21	6.22	6.18	3.63	3.87	1.27	2.6	10.54
2H-1, 0–1	6.5	6.50	3.83	3.64	1.1	2.54	9.13
2H-1, 20–21	6.7	6.68	3.942	3.39	1.19	2.2	9.88
2H-1, 40–41	6.9	6.89	4.074	3.66	1.24	2.42	10.29
2H-1, 60–61	7.1	7.09	4.199	3.8	1.31	2.49	10.87
2H-1, 80–81	7.3	7.29	4.325	3.67	1.25	2.42	10.38
2H-1, 100–101	7.5	7.49	4.45	3.35	1.07	2.28	8.88
2H-1, 120–121	7.7	7.68	4.57	3.5	1.16	2.34	9.63
2H-1, 140–141	7.9	7.89	4.702	4	1.34	2.66	11.12
2H-2, 10–11	8.14	8.10	4.835	3.93	1.4	2.53	11.62
2H-2, 30–31	8.34	8.30	4.962	4.02	1.33	2.69	11.04
2H-2, 50–51	8.54	8.50	5.088	3.51	1.2	2.31	9.96
2H-2, 70–71	8.74	8.70	5.215	3.78	1.25	2.53	10.38
2H-2, 90–91	8.94	8.86	5.317	3.52	1.11	2.41	9.21
2H-2, 110–111	9.14	9.06	5.444	3.19	0.93	2.26	7.72
2H-2, 130–131	9.34	9.26	5.571	3.34	1.1	2.24	9.13
2H-2, 149–150	9.53	9.45	5.692	3.5	1.21	2.29	10.04
2H-3, 0–1	9.54	9.44	5.686	4.97	1.04	3.93	8.63
2H-3, 20–21	9.74	9.64	5.814	2.73	0.79	1.94	6.56
2H-3, 40–41	9.94	9.82	5.929	1.63	0.45	1.18	3.74
2H-3, 61–62	10.15	10.03	6.063	1.26	0.35	0.91	2.91
2H-3, 80–81	10.34	10.22	6.185	2.62	0.85	1.77	7.06
2H-3, 100–101	10.54	10.42	6.313	3.31	1.23	2.08	10.21
2H-3, 120–121	10.74	10.62	6.442	1.28	0.3	0.98	2.49
2H-3, 140–141	10.94	10.78	6.544	3.34	1.15	2.19	9.55
2H-4, 11		11.15	10.96	6.66	3.38	1.17	2.21
2H-4, 30–31	11.35	11.14	6.776	2.87	0.91	1.96	7.55
2H-4, 50–51	11.55	11.30	6.879	3.69	1.37	2.32	11.37
2H-4, 70–71	11.75	11.49	7.002	3.44	1.17	2.27	9.71
2H-4, 90–91	11.95	11.67	7.118	3.51	1.35	2.16	11.21
2H-4, 110–111	12.15	11.82	7.215	3.36	1.24	2.12	10.29
2H-4, 130–131	12.35	12.02	7.344	3.32	1.36	1.96	11.29
2H-4, 149–150	12.54	12.21	7.467	3.19	1.38	1.81	11.45
2H-5, 0–1	12.55	12.22	7.474	3.49	1.43	2.06	11.87
2H-5, 20–21	12.75	12.36	7.564	2.92	1.06	1.86	8.8
2H-5, 40–41	12.95	12.55	7.688	3.08	1.25	1.83	10.38
2H-5, 80–81	13.35	12.86	7.889	2.77	0.91	1.86	7.55
2H-5, 100–101	13.55	13.06	8.019	1.89	0.56	1.33	4.65
2H-5, 120–121	13.75	13.24	8.136	2.87	1.08	1.79	8.96
2H-5, 140–141	13.95	13.42	8.253	3.46	1.44	2.02	11.95
2H-6, 10–11	14.15	13.59	8.364	3.6	1.48	2.12	12.28
2H-6, 30–31	14.35	13.78	8.488	3.47	1.48	1.99	12.28
2H-6, 50–51	14.55	13.93	8.586	3.24	1.31	1.93	10.87
2H-6, 70–71	14.75	14.12	8.71	2.68	0.95	1.73	7.89
2H-6, 90–91	14.95	14.32	8.841	2.44	0.87	1.57	7.22
2H-6, 110–111	15.15	14.52	8.971	2.78	1.04	1.74	8.63
2H-6, 129–130	15.34	14.71	9.096	3.21	1.31	1.9	10.87
2H-6, 148–149	15.53	14.90	9.22	2.04	0.61	1.43	5.06
2H-7, 0–1	15.55	14.91	9.227	2.93	1.24	1.69	10.29
2H-7, 20–21	15.75	15.11	9.358	3.68	1.55	2.13	12.87
2H-7, 41–42	15.96	15.32	9.496	3.4	1.42	1.98	11.79

Only the first page of this Appendix is reproduced here. The entire Appendix appears on the CD-ROM (back pocket).